

Non-Simplified SUSY: $\tilde{\tau}$ -Coannihilation at LHC and ILC

M. Berggren¹, A. Cakir¹, D. Krücker¹, J. List¹, A. Lobanov¹, I.-A. Melzer-Pellmann¹

¹DESY, Notkestraße 85, 22607 Hamburg, Germany

March 9, 2022

Simplified models have become a widely used and important tool to cover the more diverse phenomenology beyond constrained SUSY models. However, they come with a substantial number of caveats themselves, and great care needs to be taken when drawing conclusions from limits based on the simplified approach. To illustrate this issue with a concrete example, we examine the applicability of simplified model results to a series of full SUSY model points which all feature a small $\tilde{\tau}$ -LSP mass difference, and are compatible with electroweak and flavor precision observables as well as current LHC results. Various channels have been studied using the Snowmass Combined LHC detector implementation in the Delphes simulation package, as well as the Letter of Intent or Technical Design Report simulations of the ILD detector concept at the ILC. We investigated both the LHC and ILC capabilities for discovery, separation and identification of all parts of the spectrum. While parts of the spectrum would be discovered at the LHC, there is substantial room for further discoveries and property determination at the ILC.

1 Introduction

In full SUSY models, the higher states of the spectrum can have many decay modes leading to potentially long decay chains. This means that the simplified approach does in general not apply beyond the direct NLSP-production case, which renders the interpretation of exclusion limits formulated in the simplified approach non-trivial. Furthermore, also many production channels may be open, making SUSY the most serious background to itself. This becomes an issue especially for interpreting a future discovery of a non-SM signal.

We take as an example the regions in parameter space which gained the highest likelihood in fits to all pre-LHC experimental data within the constrained MSSM [1]. These fits preferred scenarios with a small mass difference of about 10 GeV between the $\tilde{\tau}$ -NLSP and the $\tilde{\chi}_1^0$ as LSP, as illustrated by the likelihood distribution in the left panel of Fig. 1. Within the context of the cMSSM, this region is ruled out by LHC searches. However this exclusion is based on the strongly interacting sector, which in constrained models is coupled to the electroweak sector by GUT-scale mass unification. Without the restriction of *mass* unification, the part of the spectrum which is of interest to electroweak and flavor precision observables and dark matter, ie. which is decisive for the fit outcome, is not at all in conflict with LHC results. This applies in particular to the $\tilde{\tau}_1$ with a small mass difference to the LSP, which is essential to allow efficient (co-)annihilation of dark matter to lower the predicted relic density to its observed value: Although first limits on direct $\tilde{\tau}$ pair production from the LHC have been presented [2, 3], they rapidly loose sensitivity if the $\tilde{\tau}$ is not degenerate with the \tilde{e} and $\tilde{\mu}$, and has a small mass difference to the LSP.

The right part of Fig. 1 shows the low mass part of an example spectrum which fulfills all constraints, including a higgs boson with SM-like branching ratios at a mass in agreement with the LHC discovery within the typical theoretical uncertainty of ± 3 GeV on MSSM higgs mass calculations. The full definition and further information can be found in [4].

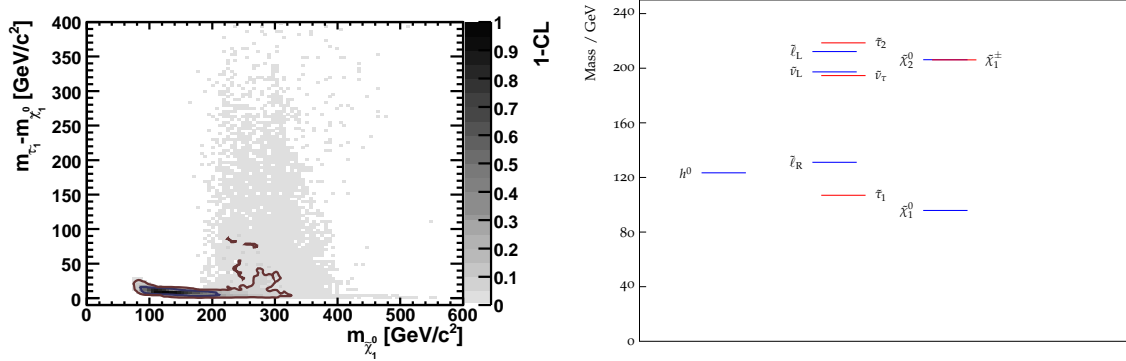


Figure 1: Left: Likelihood of a constrained MSSM fit to pre-LHC experimental data in the $\Delta M(\tilde{\tau}, \tilde{\chi}_1^0) - M_{\tilde{\chi}_1^0}$ plane, showing a clear maximum around $\Delta M(\tilde{\tau}, \tilde{\chi}_1^0) - M_{\tilde{\chi}_1^0} = 10$ GeV. From [1] Right: Lower part of the spectrum of the STC scenarios, which features $\Delta M(\tilde{\tau}, \tilde{\chi}_1^0) - M_{\tilde{\chi}_1^0} \simeq 10$ GeV.

When the 1st and 2nd generation squarks and the gluino are rather heavy, $\gtrsim 2$ TeV, the size of the total SUSY cross-section at the LHC strongly depends on the mass of the lightest top squark. We therefore consider a series of points, called STC4 to STC8, whose physical spectra differ only by the \tilde{t}_1 mass. In this series, the mass parameter of the partner of the right-handed top quark, M_{U_3} , is varied from 400 to 800 GeV at a scale of 1 TeV, resulting in $m_{\tilde{t}_1} \simeq 300\dots 700$ GeV¹.

The full spectrum of STC4 is shown in Fig. 2. The dashed lines indicate the decay chains of the various sparticles. In the left part of the figure, only decays with a branching ratio (BR) larger than 90% are shown, while the right part includes all decays with a branching fraction of at least 10%. The grey-scale of the lines indicates the size of the branching ratio. Only very few particles, namely the 1st/2nd generation squarks, the sneutrinos and the lighter set of charged sleptons have decay modes with 100% BR. In particular the stop and sbottom, but also the electroweakinos have various decay modes, none of them with a BR larger than 50%. This plethora of decay modes makes it challenging to separate the various production modes and identify each sparticle.

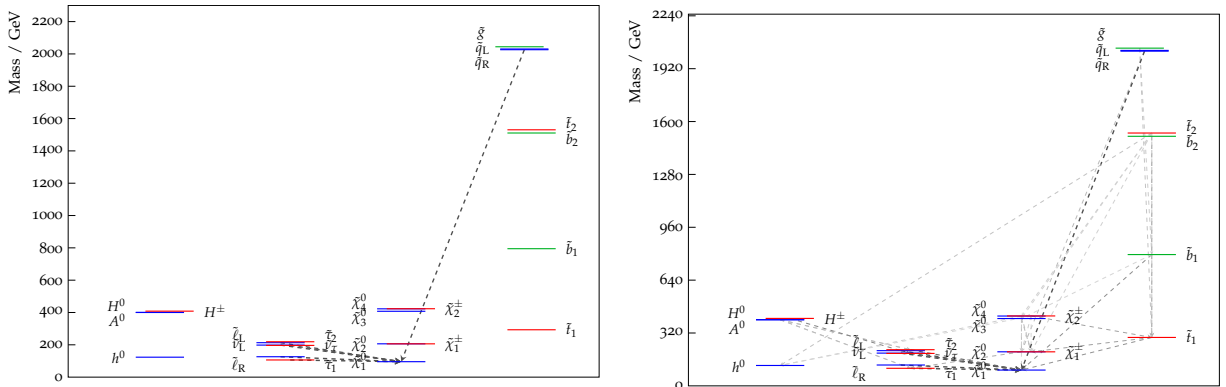


Figure 2: Left: Full spectrum of STC4, with decay modes with a branching fraction of at least 90%. Right: The same spectrum, but now indicating all decays with a branching fraction larger than 10%.

Even if not all of them can be addressed on the timescale of the Snowmass process, the final goals of this study comprise the following questions for both LHC and the ILC in the example of the STC scenarios:

- Which signature will lead to the first discovery of a discrepancy from the SM? How much integrated luminosity and operation time would be needed for this?

¹The SLHA files are available at <http://www-flc.desy.de/ldcoptimization/physics.php>.

- Which production modes of which sparticles contribute to this signal? Can we tell how many these are? And which masses and quantum numbers they have?
- Which other signatures will show a signal? And again: Can one find out which production modes contribute?
- Which observables (masses, BRs, cross-sections) can be measured with which precision?
- Can we show that it is SUSY?
- Can we show that's the MSSM (and not eg. the NMSSM)?
- Can the $\tilde{\chi}_1^0$ be identified as Dark Matter particle?

In the next section, we will describe the phenomenology of our benchmark models at the LHC and summarize the obtained simulation results. In section 3, we will do the same for the ILC case, before we give our conclusions.

2 Large Hadron Collider Studies

The discovery potential of the LHC for the STC scenarios introduced above is described in this section. Here we study the LHC at 14 TeV with 300 fb^{-1} accumulated luminosity and 50 pileup (PU) events. Next steps would be to study these scenarios with 3000 fb^{-1} and a pileup of 140 events, and a future proton-proton collider with 33 TeV.

The cross sections for the signal models have been calculated at leading order with Pythia8 [5], and for most subprocesses at next-to-leading order with Prospino2.1 [6, 7]. As Prospino offers only cross section calculations up to 14 TeV, a private patch has been applied to calculate the cross sections at 33 TeV. The inclusive cross sections for the four different models at different LHC energies are summarized in Fig. 3(a). The mass of the stop quarks rises from model STC4 to STC8 subsequently from 293 GeV to 735 GeV, reducing the cross section for stop production significantly, while the production cross section of the electroweak particles stays roughly the same. Already in STC5 the cross section for direct stop production is smaller than the one of chargino-neutralino production. The cross section of the different subprocesses for the model STC8 are shown in Fig. 3(b). A table with the cross-sections of the dominant subprocesses for all four scenarios can be found in the appendix.

The stops predominantly decay to top quarks and the lightest neutralino (54%), or to bottom quarks and the lightest chargino (46%). Here, the chargino decays mainly to $\tilde{\tau}_1$ and ν_τ (70 %) or τ and $\tilde{\nu}_\tau$ (10%), where the latter decays 93% invisibly. This situation suggests different possible strategies to search for stop production:

- In the case that both stops decay via $\tilde{t}_1 \rightarrow t\tilde{\chi}_1^0$, the $t\bar{t}$ plus missing transverse energy final state can be searched for either with no or one lepton. The sensitivity of these channels will be investigated in sections 2.2 and 2.3, respectively.
- In the case that both stops decay via $\tilde{t}_1 \rightarrow b\tilde{\chi}_1^\pm$, searches for events with two b -jets and missing transverse energy could be sensitive since the decay products of the charginos are expected to be very soft. This case has been investigated recently by ATLAS [8], and therefore we studied the event yield expected from this analysis in the case of STC4, as described in section 2.1. Due to time reasons we did not yet investigate the prospects of this analysis at 14 TeV.
- The largest branching fraction would be covered by the mixed case $\tilde{t}_1\tilde{t}_1 \rightarrow t\tilde{\chi}_1^0 b\tilde{\chi}_1^\pm$ [9]. Currently to our knowledge such a signature is not targeted by any existing LHC search. Due to time reasons we could not develop a dedicated analysis in the context of this study either, but this decay mode is expected to be covered to some extent by the fully hadronic $t\bar{t}\tilde{\chi}_1^0\tilde{\chi}_1^0$ analysis discussed in 2.2.

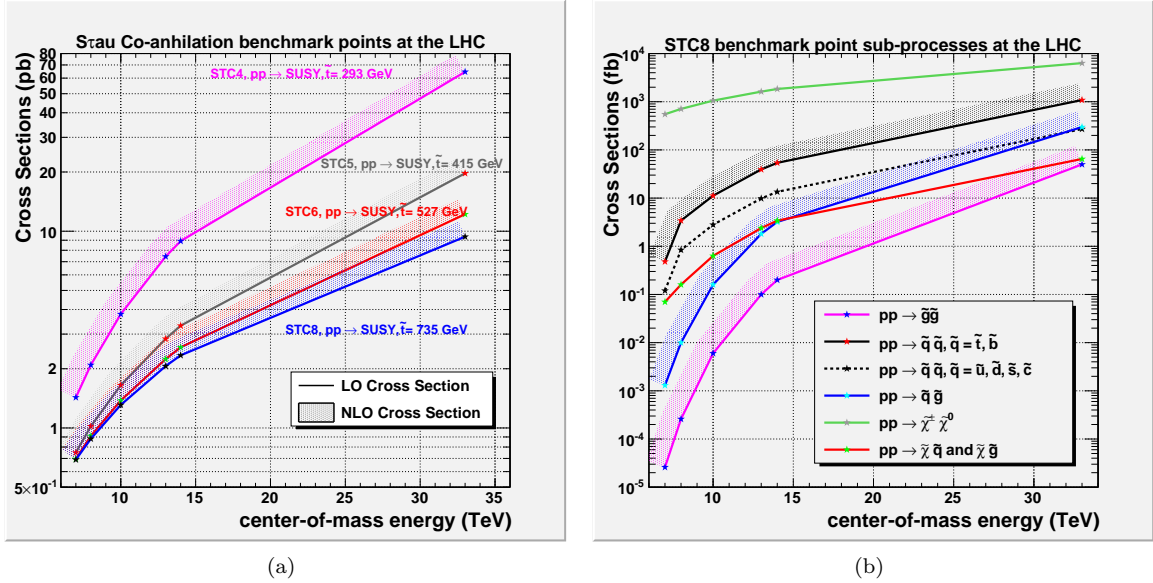


Figure 3: The inclusive cross sections of the four investigated models (a) and the cross sections of the subprocesses for the model STC8 (b). The lines correspond to the leading-order (LO) cross section and the upper end of the hatched area corresponds to the next-to-leading order (NLO) cross section.

The sbottom mass is only slightly higher than the stop mass in scenario STC8, and will be produced with almost similar cross section in this scenario. Especially the analysis of the full-hadronic final state would also be sensitive to direct sbottom production, as the sbottom decays most of the time (58%) to a bottom quark and the lightest neutralino. With high statistics (3000 fb^{-1}) it might even be possible to see slight differences in the energy spectrum of the b -tagged jets, a slightly harder spectrum is expected from the sbottom decay, but this has not yet been studied here.

The electroweak particles are very hard to identify at the LHC, as they mainly decay to final states containing rather soft tau leptons, but nevertheless we will present search prospects for electroweakino production in section 2.4.

For all analyses, signal and background are generated with Delphes 3.0.9 [10] as used by all Snowmass analyses [11, 12]. The efficiency of the reconstructed objects (muons, electrons, jets, etc.) is defined by Snowmass specific Delphes card files. In case of pileup, the fast jet correction is applied with active area correction [13]. The jet energy resolution and the resolution for the different pileup scenarios is shown in the Appendix.

While the experiments usually try to estimate the background from data to the largest possible amount, we restrict ourselves here to a simple estimation based on the simulation of the above mentioned processes.

Systematic uncertainties have been considered in terms of a conservative and an optimistic scenario, which assume global uncertainties on the background expectation of 25% and 15%, respectively, for the stop searches. The search for the electroweak particles with the same-sign analysis is expected to suffer more from the systematic uncertainties (due to the less well-known cross section of the di-boson production and analysis-specific problems like isolation in high pileup and identification of fake leptons), therefore we assume here uncertainties of 30% and 20%, respectively. For the extrapolation to 3000 fb^{-1} we expect that the systematic uncertainties will be further reduced, especially as the backgrounds are determined from data, where higher statistics will decrease the uncertainty on the background estimation. Here we assume an uncertainty of 10% for all analyses.

2.1 Comparison to 8 TeV search for final states with two b -jets

ATLAS published a search for final states with two b -jets from $\tilde{b}_1\tilde{b}_1 \rightarrow b\bar{b}\tilde{\chi}_1^0\tilde{\chi}_1^0$ based on 12.8 fb^{-1} of 8 TeV data [14]. They recently reinterpreted this analysis for $\tilde{t}_1 \rightarrow b\tilde{\chi}_1^\pm$ with small $\tilde{\chi}_1^\pm$ - $\tilde{\chi}_1^0$ mass splittings [8] based on a simplified model approach. Taking the obtained limits at face-value would lead to the conclusion that the STC4 point is excluded by this search. However, as discussed above, the concurring decay modes as well as the exact decay modes and mass splittings need to be taken into account correctly. Therefore, we reimplemented this analysis as closely as possible into the Snowmass analysis framework based on the Delphes detector simulation program and evaluated the expected signal yield for STC4 for 12.8 fb^{-1} at 8 TeV, following the selection requirements of the ATLAS analysis. We show our results in Table 1 in comparison with the experimental results from ATLAS. The signal regions SR3a and SR3b with a b -tag veto on the leading jet are not included since they are even less sensitive for our model, and we only show STC4 which has the highest stop production cross-section of our series of points. It can be easily seen from Table 1 that this ATLAS analysis is not able to exclude STC4.

Table 1: Number of signal events for the model STC4 after a selection as described for an ATLAS analysis performed on 12.8 fb^{-1} of data recorded at a center-of-mass energy of 8 TeV. The detailed cut-flow is described in the ATLAS note [14] and m_{CT} is the boost-corrected contransverse mass [15].

Description	Signal Region				
	SR1				SR2
	$m_{\text{CT}} > 150$	$m_{\text{CT}} > 200$	$m_{\text{CT}} > 250$	$m_{\text{CT}} > 300$	
ATLAS observed	172	66	16	8	104
expected SM bgrd.	176	71	25	7.4	95
95% CL UL on exp. bgrd.	55	25	12.5	5.5	32
STC4	18	13	9.0	6.6	18

2.2 Stop search with full-hadronic final states

In the followig we define a simple hadronic cut-and-count search without leptons at 14 TeV sensitive for our model points. The cut flow is summarized in Table 2. The main backgrounds in this search are:

- $t\bar{t}$ + jets
- W+jets
- Single top production
- Z+jets with $Z \rightarrow \nu\bar{\nu}$
- QCD multijet production

Several kinematic variables are exploited to separate the signal from background. We calculate the missing transverse energy E_T^{miss} as the vectorial sum of pileup subtracted jets with $p_T > 20 \text{ GeV}$ and $|\eta| < 2.5$ and leptons with $p_T > 5 \text{ GeV}$ and $|\eta| < 2.5$. Another variable to separate signal from background is the minimum angle $\Delta\Phi_{\text{min}}$ between the leading jets and E_T^{miss} , which is small for QCD multi jet background, while signal leads preferably to larger values. The scalar sum of jets with $p_T > 20 \text{ GeV}$ and $|\eta| < 2.5$ added to the missing energy, which is called $m_{\text{eff}} = H_T + E_T^{\text{miss}}$, can separate events with higher mass SUSY particles from Standard Model processes. In this analysis we use the ratio of E_T^{miss} and m_{eff} calculated with the three leading jets. After the large E_T^{miss} requirement the QCD multijet background is expected to be negligible.

The cutflow for the inclusive signal and background events for 14 TeV center-of-mass energy and 300 fb^{-1} is summarized in Table 3 for no pileup and in Table 4 for 50 pileup events.

Table 2: Overview of the event selection requirements.

Description	Selection
Lepton veto	No e or μ with $p_T > 10$ GeV
Leading jet p_T	> 120 GeV
2nd leading jet p_T	> 70 GeV
3rd leading jet p_T	> 60 GeV
No. of b-tagged jets	≥ 2
H_T	> 1000 GeV
$\Delta\Phi(E_T^{\text{miss}}, p_T^{\text{jet}1,2})$	> 0.5
$E_T^{\text{miss}}/m_{\text{eff}}$	> 0.2
E_T^{miss}	> 750 GeV

Figure 4 shows two control plots after the application of a part of the selection requirements as described in Table 2. The variable H_T is shown after the lepton veto and the jet and b-jet requirements, and E_T^{miss} after the full selection except for the E_T^{miss} requirement itself.

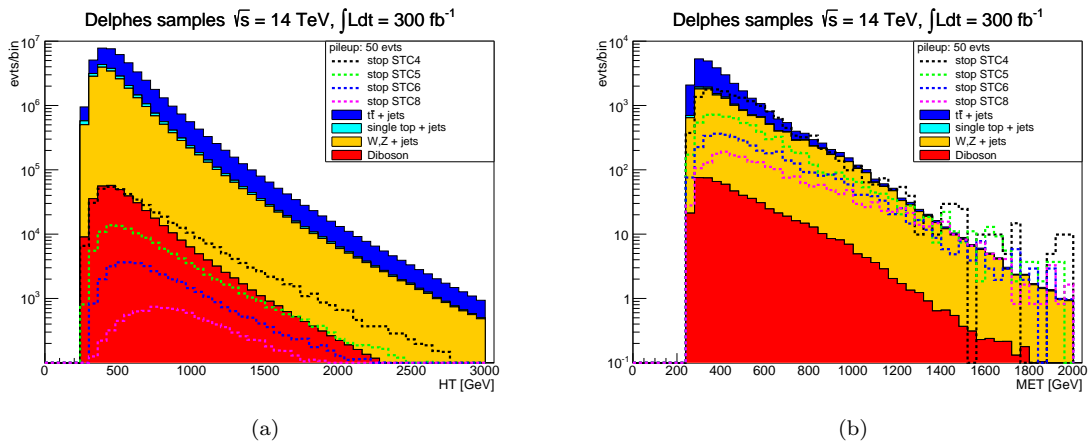


Figure 4: The scalar sum of the jets H_T after jet and b-jet requirements and lepton veto (a) and the missing transverse energy (b) after the full-hadronic event selection for 50 pileup events. The full histograms describing the backgrounds are stacked, and the four inclusive signal models are shown as dotted lines (not stacked).

We assume two cases for the systematic uncertainty: 25% and a more optimistic scenario of 15%. It is possible to see an excess due to the signal for the direct stop and sbottom production subprocess for all four scenarios, but only for STC4 and STC5 a significance of more than 3σ can be observed if the background uncertainty is around 15% or lower. Due to the smaller stop production cross section in the models STC6 and STC8 they are more challenging, as the background is higher, but it might still be possible to raise the significance if the selection and background determination is further developed. The pileup does not have a large influence here.

2.3 Stop search with final states including one electron or muon

In addition to the full-hadronic decay channel, we also investigate the discovery reach for stop decays including one electron or muon in the final state with an analysis similar to the currently performed analysis by CMS [16] on the 2012 data. The main backgrounds in this search are:

Table 3: Cutflow: number of events for the inclusive signal samples and several important backgrounds for the full-hadronic stop analyses with 300 fb^{-1} at 14 TeV without pileup. The last two lines show the significances with an additional systematic background uncertainty of 25% and, as an optimistic scenario, of 15%.

Description	diboson	ttbar+jets	boson+jets	single top	sum bgrds	STC4	STC5	STC6	STC8
preselection	110817000	215894000	16840400000	62062700	17229173700	3840000	1146000	759000	657000
lepton veto	93950100	150178000	15967400000	50836600	16262364700	2992790	867266	573276	505996
n jets ≥ 3	14108800	123304000	16122300000	22900100	1772542900	1918060	327129	106267	49223
jet1 > 120 GeV	6665570	57008900	614067000	9833780	687575250	1266390	282534	89244	35846
jet2 > 70 GeV	6102030	53676000	555486000	9053350	624317380	1177530	267671	83758	31973
jet3 > 60 GeV	4306200	43971700	351147000	6102790	405527690	962921	222022	69959	24684
bjets <i>ge2</i>	389723	24659200	21764800	2211580	49025303	551566	135976	41827	11298
$H_T > 1000 \text{ GeV}$	29056	1347070	884348	72649	2333123	67195	22797	10468	5264
$\Delta\Phi > 0.5$	19028	850594	582261	44547	1496430	40860	16951	8262	4281
$E_T^{miss}/m_{meff} > 0.2$	639	16317	14545	576	32079	16538	7486	4162	2297
$E_T^{miss} > 750 \text{ GeV}$	97	331	1908	12	2350	1843	1048	775	636
$s/\sqrt{b + (0.25 * b)^2}$						3.1	1.8	1.3	1.1
$s/\sqrt{b + (0.15 * b)^2}$						5.2	2.9	2.2	1.8

Table 4: Cutflow: number of events for the inclusive signal samples and several important backgrounds for the full-hadronic stop analyses with 300 fb^{-1} at 14 TeV and with 50 pileup events. The last two lines show the significances with an additional systematic background uncertainty of 25% and, as an optimistic scenario, of 15%.

Description	diboson	ttbar+jets	boson+jets	single top	sum bgrds	STC4	STC5	STC6	STC8
preselection	110822000	216124000	16842600000	62086200	17231632200	3840000	1146000	759000	657000
lepton veto	94040900	148709000	15970700000	50821500	16264271400	2939780	858682	569011	502994
n jets ≥ 3	15503200	118324000	19876800000	22550600	2144057800	1749960	317637	103979	48157
jet1 > 120 GeV	6945990	54696900	668990000	9576410	740209300	1052210	259433	84595	34240
jet2 > 70 GeV	6300220	51083400	597564000	8686940	663634560	960943	242314	78652	30258
jet3 > 60 GeV	4355270	41560400	359923000	5790680	411629350	774987	199271	65688	23520
bjets <i>ge2</i>	382265	23020600	21429600	2091020	46923485	433180	121225	39601	11163
$H_T > 1000 \text{ GeV}$	28432	1241760	870796	69562	2210551	59848	21130	9763	4912
$\Delta\Phi > 0.5$	18856	800289	578069	43795	1441010	36608	15623	7720	4020
$E_T^{miss}/m_{meff} > 0.2$	619	15769	12902	577	29869	15716	7067	3854	2192
$E_T^{miss} > 750 \text{ GeV}$	92	334	1721	13	2161	1920	1109	815	633
$s/\sqrt{b + (0.25 * b)^2}$						3.5	2.0	1.5	1.2
$s/\sqrt{b + (0.15 * b)^2}$						5.9	3.4	2.5	1.9

- $t\bar{t}$ + jets
- W+jets
- Single top production
- Z+jets (with one lepton not identified)

The dominant W and $t\bar{t}$ backgrounds can be controlled efficiently by analyzing the event kinematics. For this purpose two additional kinematical variables are introduced: M_T and M_{T2}^W [17]. The transverse mass, defined as

$$M_T = \sqrt{2p_T^{\text{lep}} E_T^{\text{miss}} - 2\vec{p}_T^{\text{lep}} \vec{p}_T^{\text{miss}}} \quad (1)$$

allows to reject events with leptonically decaying W bosons, while the M_{T2}^W variable, defined as the minimum 'mother' particle mass compatible with all the transverse momenta and mass-shell constraints,

$$M_{T2}^W = \text{minimum} \left\{ m_y \text{ consistent with: } \left[\begin{array}{l} \vec{p}_1^T + \vec{p}_2^T = \vec{E}_T^{\text{miss}}, p_1^2 = 0, (p_1 + p_l)^2 = p_2^2 = M_W^2, \\ (p_1 + p_l + p_{b_1})^2 = (p_2 + p_{b_2})^2 = m_y^2 \end{array} \right] \right\}. \quad (2)$$

exploits the event topology to reject semileptonic $t\bar{t}$ events. By construction, M_{T2}^W has an endpoint at the top mass for the dilepton $t\bar{t}$ background.

For events with two identified b jets the calculation relies on the correct pairing of the lepton and the b jets. For events with only one identified b jet one of the none b -tagged jets has to be included. The definition 2 is therefore extended by minimizing over all possible lepton, jet, and b -jet combinations within an event.

The missing transverse energy E_T^{miss} is calculated as for the fully hadronic case 2.2, and similar the minimum angle $\Delta\Phi_{\text{min}}$ which is now calculated for only the two highest p_T jets.

An overview of the event selection is given in Table 5. A cutflow with these requirements is given in Table 6 for no pileup and in Table 7 for 50 pileup events. Figure 5 contains the M_T distribution after all lepton and jet requirements (a) and the lepton transverse momentum (b) after the M_T requirement.

Table 5: Overview of the event selection requirements for the leptonic direct stop search.

Description	Selection
Exactly 1 lepton	e or μ with $p_T > 30$ GeV no other e/μ with $p_T > 10$ GeV
Number of jets	$n \geq 4$ with $p_T > 40$ GeV
b -tagged jets	1 or 2
$\Delta\Phi(E_T^{\text{miss}}, p_T^{\text{jet}1,2})$	> 0.5
E_T^{miss}	> 500 GeV
H_T	> 500 GeV
M_T	> 120 GeV
$M_{T2}^W > 250$ GeV	topness > 9.5 p_T asymmetry > -0.2

As an alternative to M_{T2}^W for suppressing the dileptonic top background we consider the *topness* variable as defined in [9]. The unknown lepton momenta, i.e. the lost electron or muon and the two neutrinos, are reconstructed by numerically minimizing a χ^2 -expression that also takes into account the invariant mass of the $t\bar{t}$ system. We have applied the different parameters, i.e. resolution terms, as given in [9] and did not optimized for the 14 TeV and high pileup case. We also cut on the p_T asymmetry between the lepton and the leading b jet

$$p_T \text{ asymmetry} = \frac{p_T^{\text{b-jet}} - p_T^{\text{lep}}}{p_T^{\text{b-jet}} + p_T^{\text{lep}}}. \quad (3)$$

In Table 7 both methods are compared for the case of 50 pileup events. Topness in general performances well. Typically, it has a higher selection efficiency compared to M_{T2}^W and improves the discovery potential (section 2.5) in most cases.

All the above kinematic variables are sensitive to pileup but the sensitivity can be mitigated by adjusting the jet and lepton p_T cuts. The high momentum lepton from the stop decay provides an additional handle to select stop decays in a high pileup environment. After all selection requirements, the analysis is sensitive to all four models with 300 fb^{-1} . While this analysis, containing one lepton which is expected to originate from a top decay, is especially sensitive to decays containing top quarks, the full-hadronic analysis is also sensitive to decays containing only bottom decays. By comparison of these two analyses it will be possible to draw some conclusion on whether a stop or sbottom decay is observed in data.

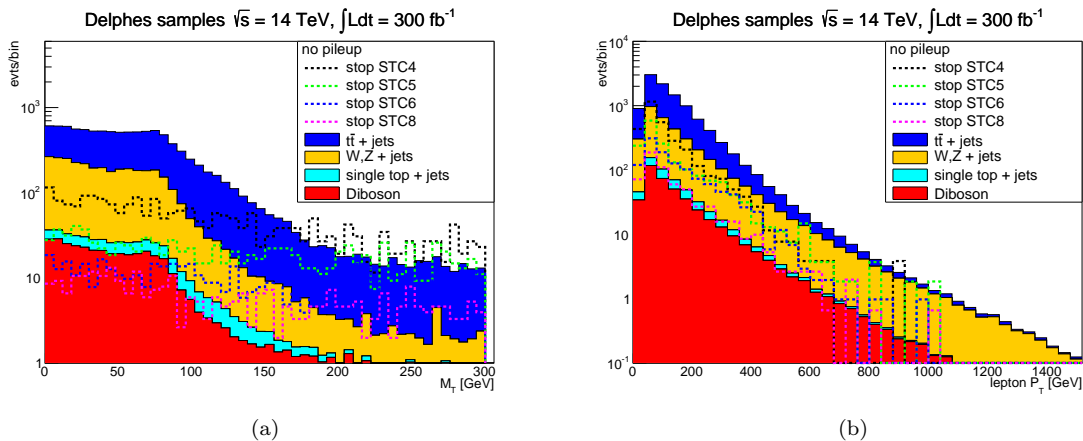


Figure 5: M_T distribution after all lepton and jet requirements (a) and the lepton transverse momentum (b) after the M_T requirement. The full histograms describing the backgrounds are stacked, and the inclusive signals for all four models are shown as dotted lines (not stacked).

2.4 Search for decays of the electroweak subprocess $pp \rightarrow \tilde{\chi}_1^\pm \tilde{\chi}_2^0$

Once stop production is discovered, it needs to be clarified whether the stops are accompanied by sleptons and/or electroweak bosinos, which could very well hide at lower masses. Therefore, we study here the possibility to explore the electroweak spectrum of the investigated models. Current analyses [18, 19] do not have the power to see any of the four studied models, as the processes of interest cannot be excluded by simplified models that assume a 100% branching ratio of $\tilde{\chi}_1^\pm \rightarrow \tilde{\tau} \nu_\tau$ and of $\tilde{\chi}_2^0 \rightarrow \tilde{\tau} \tau$, where the $\tilde{\tau}$ mass is defined as $m_{\tilde{\tau}} = 0.5m_{\tilde{\chi}_1^\pm} + 0.5m_{\tilde{\chi}_2^0}$. Models where the $\tilde{\tau}$ mass is closer to the $\tilde{\chi}_1^0$ are in general more difficult, as the final objects are softer.

We are here investigating a final state containing two same-sign leptons, where only electrons and muons are taken into account. These are expected in case of leptonic τ decays of the above particles, where one lepton of the $\tilde{\chi}_2^0$ decay is lost, and the other one has the same charge as the lepton from the $\tilde{\chi}_1^\pm$ decay. The lepton is softer than in the previous analysis, as can be seen from Fig. 6, which displays the transverse momentum of the leading lepton of the same-sign pair.

The main backgrounds originate from (di-)vectorboson+jets events. Background from $t\bar{t}$ can rarely occur from dileptonic decays, where the charge of an electron is reconstructed wrongly (we did not study whether such effects are simulated properly in Delphes), or from semileptonic top decays, where a second lepton originates from the b decay and is (in rare cases) isolated. Typically, such a background can be reduced by tightening the isolation criterium, which is not possible for the Snowmass Delphes samples. Also $t\bar{t}$ production in association with a vectorboson can lead to a same-sign signature. All backgrounds containing

Table 6: Outflow: number of events for the inclusive signal samples and several important backgrounds for the single-lepton stop analyses with 300 fb⁻¹ at 14 TeV without pileup. The last two lines show the significances with an additional systematic background uncertainty of 25% and, as an optimistic scenario, of 15%.

Description	diboson	ttbar+jets	boson+jets	single top	sum bgrds	STC4	STC5	STC6	STC8
preselection	110817000	215894000	16840400000	62062700	17229173700	3840000	1146000	759000	657000
singl. lep. and τ veto	9910050	40839900	552664000	7768710	611182660	431923	112517	63185	46360
n jets ≥ 4	253994	10916500	4208940	166321	15539755	166663	33967	12546	4136
b-tagged jets = 1 or 2	91026	8727330	1225930	131791	10176077	134556	26899	9141	2411
$E_T^{\text{miss}} > 500$ GeV	383	6552	2784	130	9852	2246	1282	903	423
$\Delta\Phi > 0.5$	358	5779	2612	111	8861	1682	1054	783	375
$H_T > 1500$ GeV	49	622	366	12	1051	460	282	214	147
$M_T > 120$ GeV	6	108	21	1	137	273	176	141	101
topness > 9.5 and p_T asym. < -0.2	4	61	12	1	79	168	124	111	85
$s/\sqrt{b+(0.25*b)^2}$						7.7	5.7	5.1	3.9
$s/\sqrt{b+(0.15*b)^2}$						11.3	8.3	7.5	5.7

Table 7: Outflow: number of events for the inclusive signal samples and several important backgrounds for the single-lepton stop analyses with 300 fb⁻¹ at 14 TeV and with 50 pileup events. The last two lines show the significances with an additional systematic background uncertainty of 25% and, as an optimistic scenario, of 15%. Also shown is an example for the differences between the *topness* based selection and the M_{T2}^W approach.

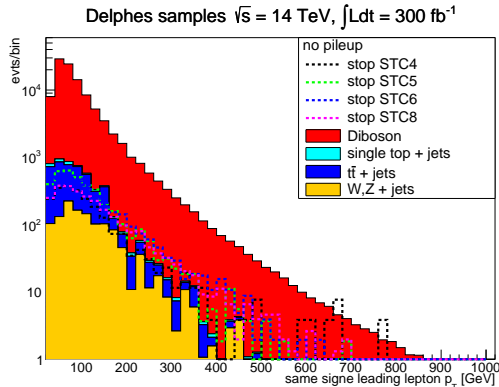
Description	diboson	ttbar+jets	boson+jets	single top	sum bgrds	STC4	STC5	STC6	STC8
preselection	110822000	216124000	16842600000	62086200	17231632200	3840000	1146000	759000	657000
singl. lep. and τ veto	9652070	40031600	536493000	7465180	593641850	427551	110574	61849	45070
n jets ≥ 4	277933	10210600	5009660	181852	15680045	155328	34542	13211	4300
b-tagged jets = 1 or 2	96490	8161060	1388700	148269	9794519	122321	26681	9285	2416
$E_T^{\text{miss}} > 500$ GeV	384	6776	2920	145	10227	2434	1286	855	414
$\Delta\Phi > 0.5$	356	5968	2733	123	9181	1725	1057	751	370
$H_T > 1500$ GeV	49	640	374	12	1076	492	277	209	129
$M_T > 120$ GeV	6	110	25	1	143	269	162	140	85
$M_{T2}^W > 250$ GeV	4	52	19	0	77	116	79	102	62
$s/\sqrt{b+(0.25*b)^2}$						5.5	3.7	4.8	2.9
$s/\sqrt{b+(0.15*b)^2}$						8.0	5.5	7.0	4.3
topness > 9.5 and p_T asym. < -0.2	4	62	15	1	83	155	98	107	67
$s/\sqrt{b+(0.25*b)^2}$						6.9	4.3	4.7	3.0
$s/\sqrt{b+(0.15*b)^2}$						10.1	6.4	6.9	4.3

Table 8: Cutflow: number of events for the inclusive signal samples and several important backgrounds for the same-sign di-lepton analysis targeting electroweak particles with 300 fb^{-1} at 14 TeV and without pileup. The last two lines show the significances with an additional systematic background uncertainty of 30% and, as an optimistic scenario, of 20%.

Description	diboson	ttbar+jets	boson+jets	single top	sum bgrds	STC4	STC5	STC6	STC8
preselection	110817000	215894000	16840400000	62062700	17229173700	3840000	1146000	759000	657000
2 lepton req.	2001300	6362250	53165400	7180	61536130	72024	38810	30136	23439
$E_T^{miss} > 120 \text{ GeV}$	111344	1005900	686304	872	1804420	35841	21353	16059	11472
same-sign req.	7126	741	536	105	8510	1264	2431	2254	1625
Z veto	3021	731	390	104	4247	1015	1975	1801	1323
b-jet veto	2640	98	304	46	3091	729	957	851	730
$E_T^{miss} > 200 \text{ GeV}$	738	43	89	12	883	408	512	474	411
$E_T^{miss} > 400 \text{ GeV}$	88	4	17	0	110	86	116	131	115
$s/\sqrt{b + (0.3 * b)^2}$						2.5	3.3	3.8	3.3
$s/\sqrt{b + (0.2 * b)^2}$						3.5	4.7	5.3	4.7

Table 9: Cutflow: number of events for the inclusive signal samples and several important backgrounds for the same-sign di-lepton analysis targeting electroweak particles with 300 fb^{-1} at 14 TeV and with 50 pileup events. The last two lines show the significances with an additional systematic background uncertainty of 30% and, as an optimistic scenario, of 20%.

Description	diboson	ttbar+jets	boson+jets	single top	sum bgrds	STC4	STC5	STC6	STC8
preselection	110822000	216124000	16842600000	62086200	17231632200	3840000	1146000	759000	657000
2 lepton req.	1914290	6745420	50864800	66503	59591013	80459	40117	30936	23903
$E_T^{miss} > 120 \text{ GeV}$	125330	1203360	883404	8527	2220621	39799	22116	16700	11604
same-sign req.	7920	7424	2511	548	18405	1385	2431	2284	1659
Z veto	3546	7356	2115	546	13565	1121	1988	1829	1335
b-jet veto	3071	2183	1172	201	6629	701	930	838	740
$E_T^{miss} > 200 \text{ GeV}$	783	413	414	46	1657	378	526	460	424
$E_T^{miss} > 400 \text{ GeV}$	90	21	66	3	182	91	109	114	101
$s/\sqrt{b + (0.3 * b)^2}$						1.6	1.9	2.0	1.8
$s/\sqrt{b + (0.2 * b)^2}$						2.4	2.8	2.9	2.6



(a)

Figure 6: The lepton transverse momentum of the leading lepton of the same-sign pair in the electroweakino analysis. The full histograms describing the backgrounds are stacked, and the four inclusive signal models are shown as dotted lines (not stacked).

Z bosons are reduced by rejecting events that, after applying looser electron and muon selection criteria, contain an OSSF pair within 15 GeV of the Z boson mass (Z -veto).

Tables 8 and 9 summarize the expected number of events for this analysis at the LHC with a center-of-mass energy of 14 TeV and an integrated luminosity of 300 fb^{-1} . After the requirement of two same-sign leptons, the SM background is strongly reduced, though this effect is reduced in the case with 50 pileup events. The number of events in the signal regions differ for the different models. The difference is reduced if one requires zero b-tags, but then the significance of the signal is reduced as well. The b-tag requirement renders a clean electroweakino signal, as can be seen by the fact that final event yields for all model points are similar. The expected systematic uncertainty is worse for this analysis compared to the stop analyses in current data, therefore we assume a larger uncertainty also for 300 fb^{-1} .

In summary, the signal is at the edge of visibility, and a 5σ discovery requires an understanding of the background to better than 5%. A deviation from the analysis design from [18], can improve the sensitivity for our signal points but probably only at the cost of a higher stop contamination. Once a signal is observed, the selection requirements would have to be developed further, and also 3-lepton final states should be taken into account to enhance the significance. If more than the expected number of events are observed with this analysis, it would be a hint for additional electroweak production, which then could be determined further at the ILC. But based on the current studies, it could also be possible that the electroweakinos remain buried below the background and its systematics. This is an example where the ILC would serve as discovery machine, and with its precise measurements could help to narrow the LHC analyses such that a signal could also be extracted from the LHC data.

2.5 LHC projections in view of luminosity and systematic uncertainties

In this section we summarize the results of the three performed analyses (in the case of 50 pileup events) and compare the sensitivity (in terms of standard deviations σ) for exclusion or discovery of the STC models. We use the observed number of events as test statistics, corresponding to a pure counting experiment. A discovery with a certain significance can be claimed if the background-only hypothesis can be excluded at this significance:

$$\sigma_{disc} = S/\sqrt{B + (\delta B_{sys})^2} \quad (4)$$

Here, S and B are the respective numbers of events expected for signal and (SM) background at a certain integrated luminosity. The significance for exclusion of the signal-plus-background hypothesis is defined analogously, but replacing B by $S + B$ in the above formula.

As already indicated in the cutflow tables, the assumptions on how well systematic uncertainties can be controlled will be decisive. Figure 7 shows the discovery and exclusion sensitivities as a function of the relative systematic uncertainty, based on an integrated luminosity fixed to 300 fb^{-1} . It leads to the following observations²:

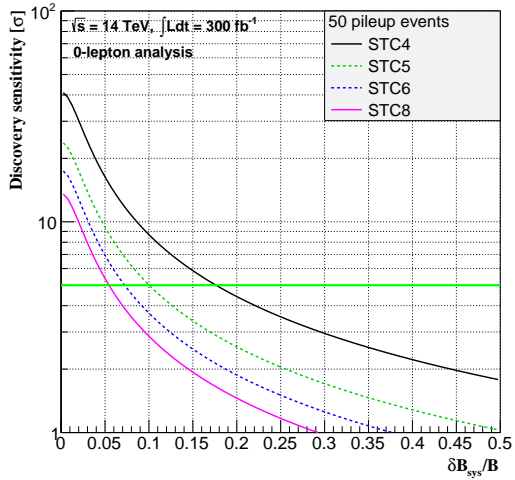
- Already at 300 fb^{-1} , all three searches are limited by systematics in all scenarios.
- The 1-lepton analysis as the cleanest selection is the most robust one against systematic uncertainties, but also this search is systematically limited for uncertainties larger than 10%.
- The 1-lepton analysis can discover the STC4, STC5 and STC6 scenarios with at least 5σ if the systematics can be controlled better than 20% to 35%. Discovery of STC8 needs precision better than 12%.
- In case of the 0-lepton analysis, systematic uncertainties smaller than 18% (STC4) to 5% (STC8) are needed for a 5σ discovery. However in case of small systematics, potentially much larger sensitivities can be reached than with the 1-lepton analysis.
- The same-sign di-lepton analysis is most fragile with respect to systematic uncertainties. Exclusion or discovery requires a control of the systematics to at least 10% or 7%, respectively.
- In case of the same-sign di-lepton, the sensitivity is very similar for all four scenarios, remaining differences reflect the available MC statistics. This demonstrates that indeed the same-sign di-lepton analysis selects electroweakino production, which is the same in all four scenarios, with rather little contamination by the strongly varying stop production.

Figure 8 shows the discovery sensitivity of all three analyses as a function of the integrated luminosity for two different assumptions on the systematic uncertainties: 25% or 15% (30% or 20% for the 2-lepton analysis). Sensitivity numbers for additional values of the systematic uncertainty can be found in the cutflow tables. A thorough estimate of the achievable precision for each analysis is beyond the scope of this study, so we leave it to the judgement of the reader which scenario to consider the most realistic. We draw the following conclusions:

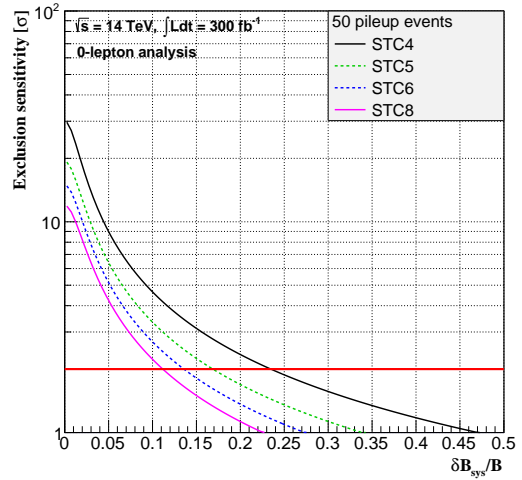
- In case of 25% systematic uncertainty, the 1-lepton analysis will be the first – and only – analysis which allows a stand-alone 5σ discovery of STC4 after accumulating 45 fb^{-1} . STC5 and STC6 are at the edge of discovery.
- In all other scenarios and analyses no 5σ discovery is possible assuming an uncertainty of 25%, even with 3000 fb^{-1} .
- Assuming a modelling of all backgrounds at the level of 15% is possible, the first discovery will move to the 0-lepton analysis in case of STC4, requiring not even 15 fb^{-1} at 14 TeV!
- Staying with 15% systematic uncertainty, STC5 and STC6 would be first discovered in the 1-lepton search after accumulating 100 fb^{-1} .
- STC8 would first – and only – be discovered in the 1-lepton analysis with 1000 fb^{-1} , again assuming a systematic uncertainty of 15%.
- No analysis would gain significantly from a luminosity increase to 3000 fb^{-1} . Only the 1-lepton analysis may improve, if the systematic uncertainties can be controlled beyond the 15% level.

Figure 9 finally gives the same set of plots for the case of exclusion sensitivity.

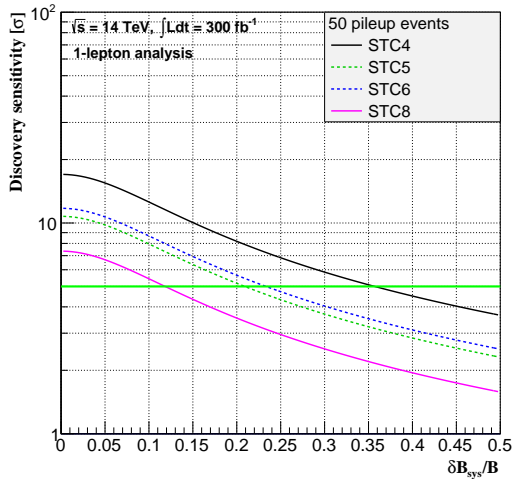
²The statistical uncertainty of these results are dominated by the statistical uncertainty of our signal samples which is typically in the order of 10%.



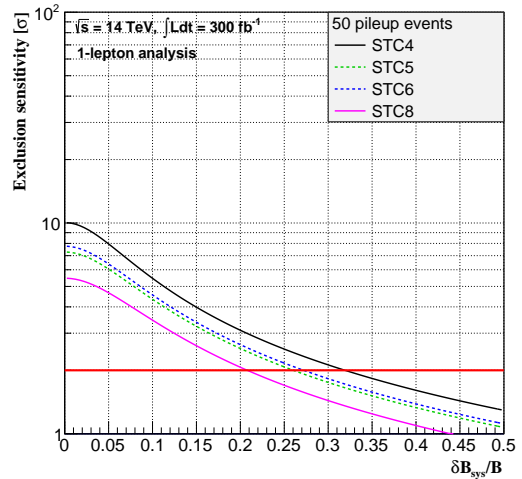
(a) 0-lepton analysis, discovery sensitivity



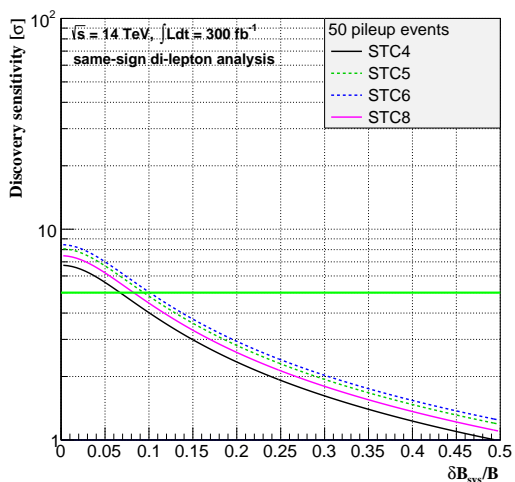
(b) 0-lepton analysis, exclusion sensitivity



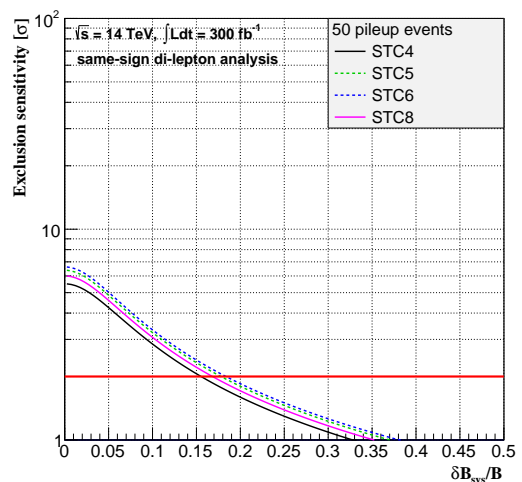
(c) 1-lepton analysis, discovery sensitivity



(d) 1-lepton analysis, exclusion sensitivity

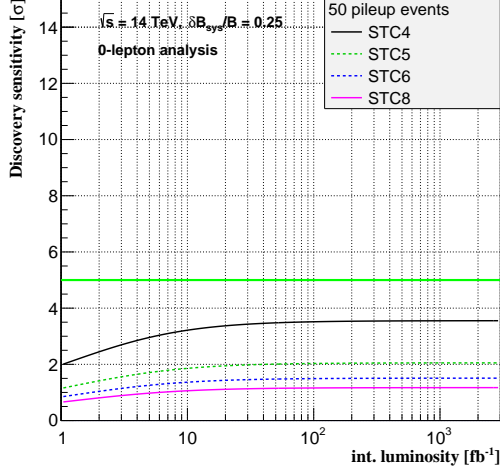


(e) 2-lepton analysis, discovery sensitivity

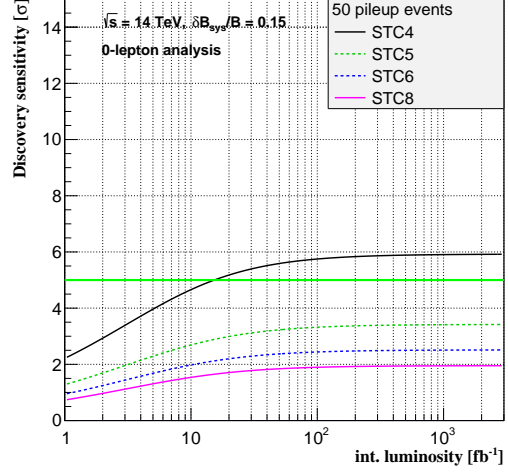


(f) 2-lepton analysis, exclusion sensitivity

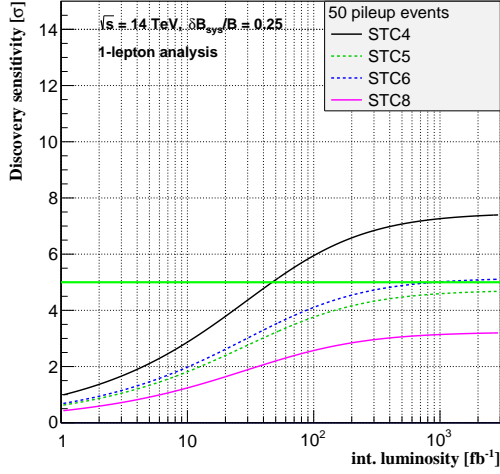
Figure 7: (a),(c),(e): Discovery significances for the 4 STC models by the 3 considered analyses as a function of the relative systematic uncertainty on the background. The green horizontal line indicates the 5- σ -level. (b),(d),(f): Same for the exclusion sensitivity - the red horizontal line indicates the 2- σ -level (ie. exclusion at 95% CL).



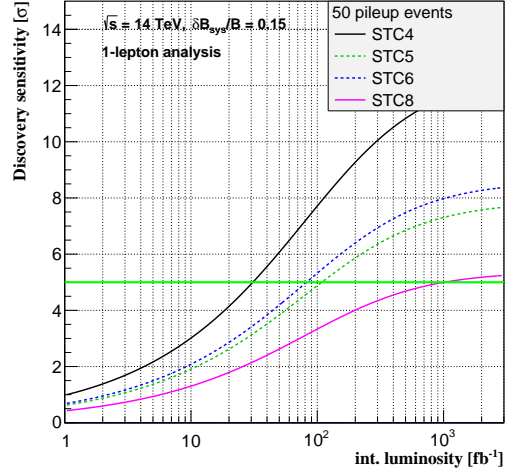
(a) 0-lepton analysis, 25% uncertainty



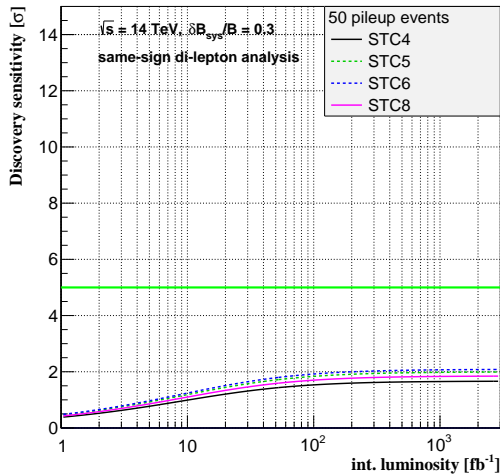
(b) 0-lepton analysis, 15% uncertainty



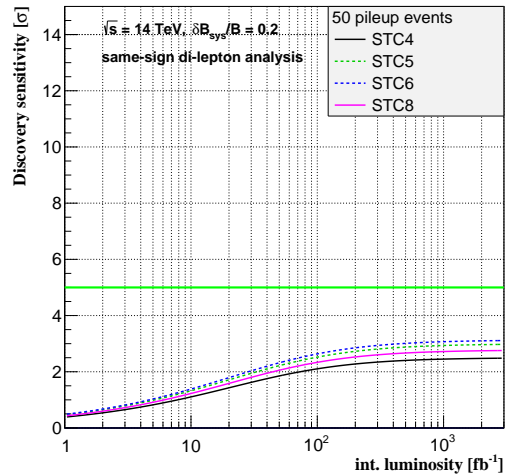
(c) 1-lepton analysis, 25% uncertainty



(d) 1-lepton analysis, 15% uncertainty

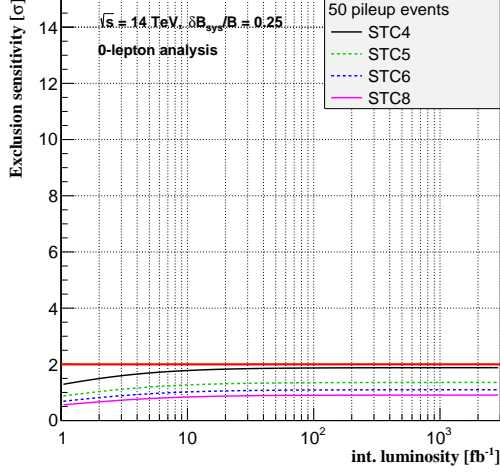


(e) 2-lepton analysis, 30% uncertainty

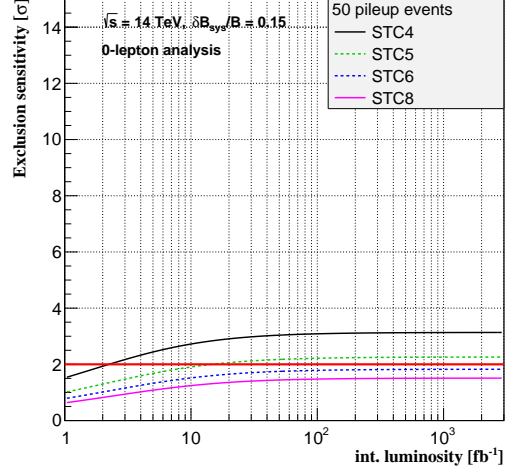


(f) 2-lepton analysis, 20% uncertainty

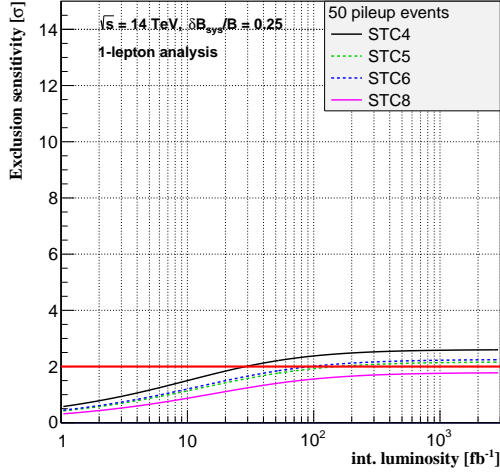
Figure 8: (a),(c),(e): Discovery significances for the 4 STC models by the 3 considered analyses as a function of the integrated luminosity assuming a relative systematic uncertainty of 25%(30%) on the background. (b),(d),(f): Same but assuming a reduced systematic uncertainty of 15%(20%). The green horizontal line indicates the 5- σ -level.



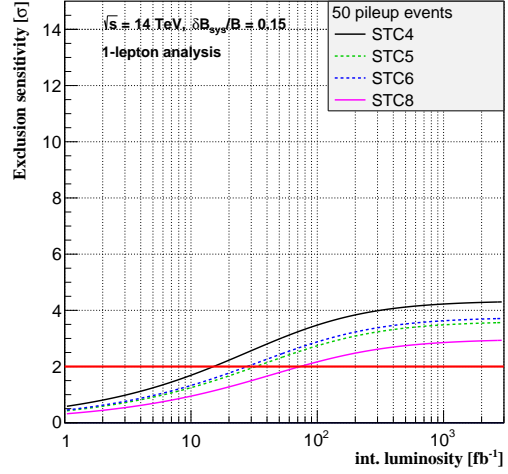
(a) 0-lepton analysis, 25% uncertainty



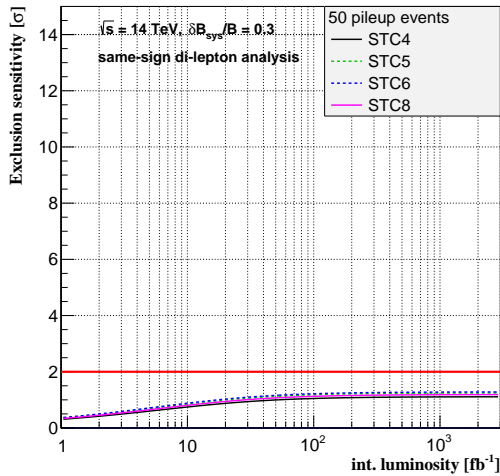
(b) 0-lepton analysis, 15% uncertainty



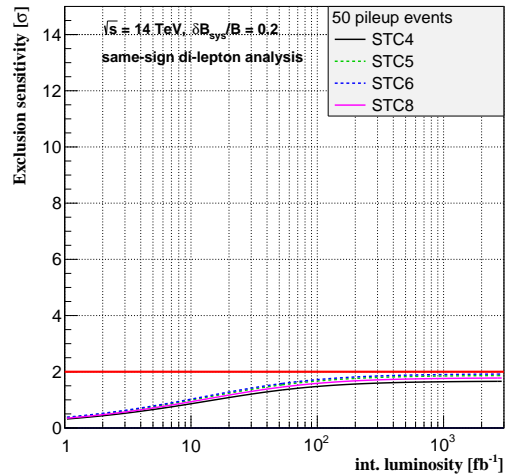
(c) 1-lepton analysis, 25% uncertainty



(d) 1-lepton analysis, 15% uncertainty



(e) 2-lepton analysis, 30% uncertainty



(f) 2-lepton analysis, 20% uncertainty

Figure 9: (a),(c),(e): Exclusion significances for the 4 STC models by the 3 considered analyses as a function of the integrated luminosity assuming a relative systematic uncertainty of 25%(30%) on the background. (b),(d),(f): Same but assuming a reduced systematic uncertainty of 15%(20%). The red horizontal line indicates the $2\text{-}\sigma$ -level (ie. exclusion at 95% CL). 16

- In case of a systematic uncertainty of 15%, all models can be excluded by the 1-lepton analysis, and with the exception of STC6 and STC8 in the 0-lepton analysis. The required integrated luminosities for exclusion at 95% CL range from less than 2 fb^{-1} (STC4, 0-lepton) to a few 100 fb^{-1} .
- The electroweakino sector of the STC models cannot be excluded with any amount of integrated luminosity, including 3000 fb^{-1} .
- The stop sector of STC4 would be excluded by the 0-lepton analysis, requiring only little more than 2 fb^{-1} (15% systematics).
- Stop production in STC5 and STC6 would be first excluded by the 1-lepton analysis with 30 fb^{-1} (again 15% systematics). STC8 could be excluded at 80 fb^{-1} in this case.
- In case of 25% systematics, STC8 would not be excluded by any of the analyses at any luminosity.

Of course these results are based on only three cut based analyses which could be implemented and roughly optimised during the time available with respect to the Snowmass study. Further optimisation is most probably possible. With increasing luminosity, the optimal working point of the analyses is likely to be found for harder cuts, since a purer selection is less vulnerable to systematic uncertainties. On the other hand this means cutting further out in the tails of distributions, where the relative systematic uncertainties might be larger. It should also be noted that the extrapolation to 3000 fb^{-1} is done here under the assumption of 50 pileup events³.

Nevertheless the potentially large impact of systematic uncertainties on the discovery of difficult signatures should be taken note of. At some point, better control of backgrounds might be more important than increase in luminosity. Furthermore precise knowledge of the lower lying states (e.g. the EWKinos, but also the sleptons) from a Linear Collider could predict the decay chains of the heavy states, including their kinematics, and thus give important input to the study of the heavier states (e.g. stop /sbottom) at the LHC.

3 International Linear Collider Studies

At the ILC running at $E_{\text{cms}} = 500 \text{ GeV}$, all sleptons and the lighter set of electroweakinos of the STC scenarios can be produced. $\tilde{\chi}_3^0$ and $\tilde{\chi}_4^0$ become accessible in associated production around $E_{\text{cms}} = 600 \text{ GeV}$ and in pair production at around $E_{\text{cms}} = 850 \text{ GeV}$, along with $\tilde{\chi}_2^\pm$ pair production. The cross sections are sizable – only one of the kinematically allowed processes would have a production cross section below 1 fb for both beam polarization configurations. The total SUSY cross section is over 3 pb in both cases. Figure 10 shows the polarized cross sections for various processes as a function of the center-of-mass energy in linear and logarithmic scale.

Although the $\tilde{\tau}_1$ is the NLSP, almost all electroweakinos have sizable branching fractions to other final states than the notoriously difficult τ -lepton. This also means that signatures with electrons or muons in the final state can originate either from slepton or electroweakino production. The ability to operate at any desired center-of-mass energy between 200 and 500 GeV (or even 1 TeV) and to switch the sign of the beam polarizations are unique tools to identify each of these processes. The low SM background levels allow in many cases a full and unique kinematic reconstruction of cascade decays.

3.1 First observation channels

The first channel to manifest itself at the ILC depends on the assumed running scenario. If the ILC starts out as a Higgs factory at $E_{\text{cms}} = 250 \text{ GeV}$, then $e^+e^- \rightarrow \tilde{\tau}_1\tilde{\tau}_1$ and $\tilde{\chi}_1^0\tilde{\chi}_1^0\gamma$ would be the first observable channels, while \tilde{e}_R and $\tilde{\mu}_R$ pair production is just beyond reach. The measurement of the $\tilde{\tau}$ mass however

³Results for simulations with 140 pileup events are given in the appendix.

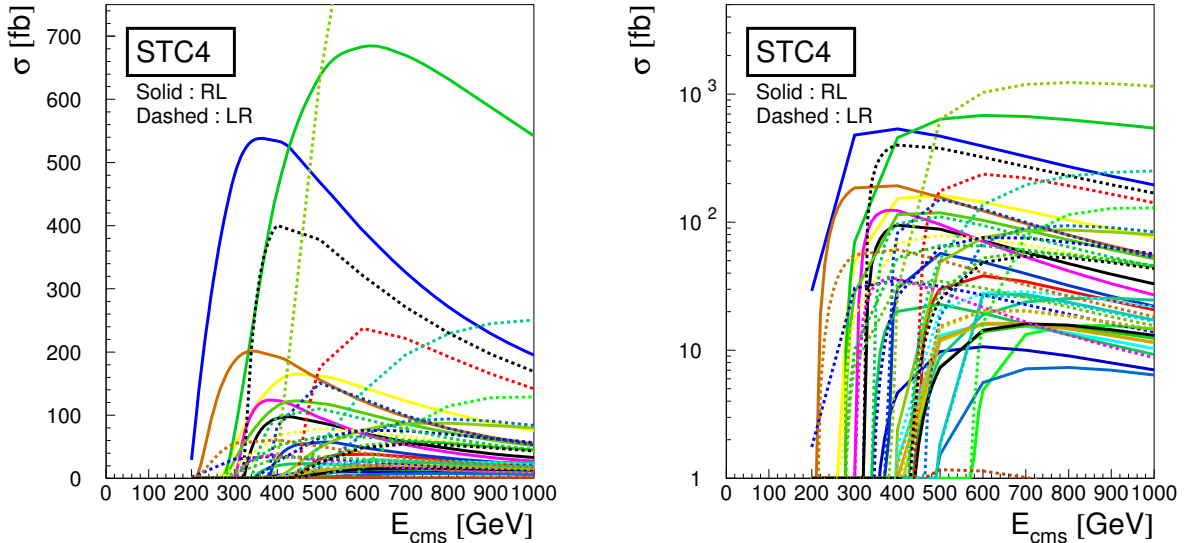


Figure 10: STC4 cross sections for sparticle production as a function of E_{cms} at the ILC. Full lines correspond to $P(e^+e^-) = (-0.3, +0.8)$, dashed lines to $P(e^+e^-) = (-0.3, +0.8)$. Left: linear scale; Right: logarithmic scale. The most prominent channels at $P(e^+e^-) = (-0.3, +0.8)$ are $\tilde{\chi}_1^0\tilde{\chi}_1^0$ (blue), $\tilde{e}_R\tilde{e}_R$ (green), $\tilde{\tau}_1\tilde{\tau}_1$ (brown), and $\tilde{\chi}_1^0\tilde{\chi}_2^0$ (yellow). At $P(e^+e^-) = (-0.3, +0.8)$ they are $\tilde{\nu}_e\tilde{\nu}_e$ (olive green), $\tilde{\chi}_1^+\tilde{\chi}_1^-$ (black), $\tilde{\chi}_1^\pm\tilde{\chi}_2^\pm$ (red), and $\tilde{e}_L\tilde{e}_L$ (blue-green).

would be challenging close to threshold, since both upper and lower edge of the τ -lepton energy spectrum would be in the region affected by background from multi-peripheral two-photon processes.

On the other hand, the LSP mass and pair production cross-section could be measured at least with a few percent precision from the energy (or recoil mass) spectrum of the accompanying ISR photons [22]. The left part of Fig. 11 illustrates the precision achievable on the neutralino mass from a template fit⁴. Since the neutralino pair production is dominated by t -channel selectron exchange, the mass of the lighter selectron and its helicity can be determined from the measurement of the polarized cross-sections.

As soon as the center-of-mass energy is raised past the pair production threshold for right-handed sleptons, in our case when $E_{\text{cms}} \gtrsim 270$ GeV, the $e^+e^- + \text{missing 4-momentum}$ signature would see a striking signal within a few days. Figure 11 shows the SM and all SUSY contributions to this signature after a simple event selection on just 10 fb^{-1} of data at $E_{\text{cms}} = 500$ GeV, which corresponds to one week of data taking at design luminosity.

The cross-section for $\tilde{\mu}_R$ pair production is much lower due to the absence of a t -channel. Still the $\tilde{\mu}_R$ mass can be determined to ~ 200 MeV by scanning the production threshold near 270 GeV [23], as illustrated by Fig. 12. Note that this can be improved to ~ 10 MeV in the continuum if $\tilde{\chi}_2^0\tilde{\chi}_2^0$ is accessible and $\tilde{\chi}_2^0$ has a non-vanishing branching fraction to $\tilde{\mu}_R\mu$, cf. below.

3.2 Sleptons and Electroweakinos in the Continuum

Several of the channels in the slepton and electroweakino sector are being studied, or have been in the past in very similar models, assuming only a moderate amount of integrated luminosity of 500 fb^{-1} at $E_{\text{cms}} = 500$ GeV unless stated otherwise. This corresponds to two years of ILC operation at design parameters.

⁴This study has been performed at a higher center-of-mass energy. At $E_{\text{cms}} = 250$ GeV, the cross-section is similar, and the photon energy spectrum less spread out, so that the quality of the mass determination is expected to be comparable.

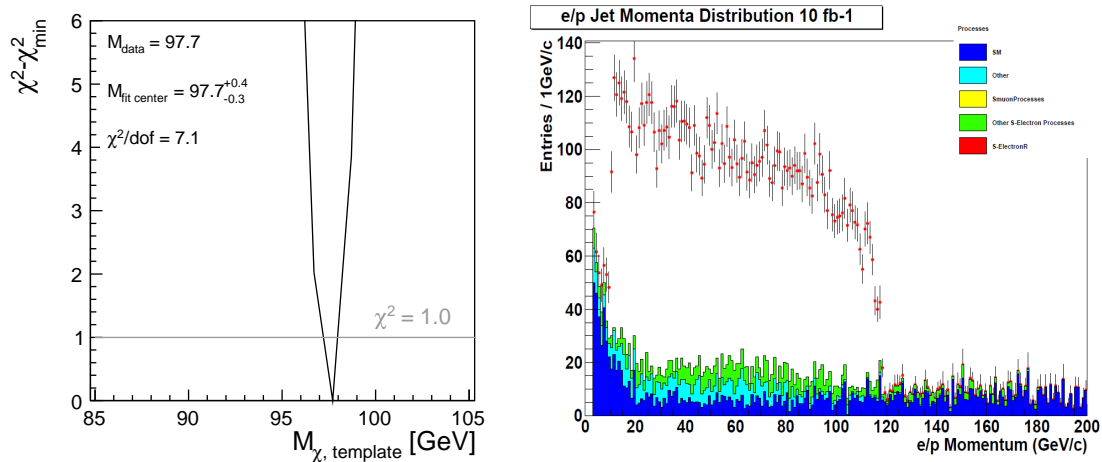


Figure 11: Left: Determination of $m_{\tilde{\chi}_1^0}$ from a template fit to the photon energy spectrum in $e^+e^- \rightarrow \tilde{\chi}_1^0 \tilde{\chi}_1^0 \gamma$. From [20]. Right: Momentum spectrum of events with e^+e^- and missing 4-momentum. The assumed luminosity of 10 fb^{-1} corresponds to one week data taking at design luminosity. From [21].

3.2.1 The $\tilde{\tau}$ -Sector

Especially in $\tilde{\tau}$ -coannihilation scenarios, a precise determination of the $\tilde{\tau}$ sector is essential in order to be able to predict the expected relic density with sufficient precision to test whether the $\tilde{\chi}_1^0$ is indeed the dominant Dark Matter constituent. The capabilities for precision measurements in the $\tilde{\tau}$ sector have been studied in full detector simulation [24]. It was shown that the $\tilde{\tau}_1$ mass could be determined to 200 MeV, and the $\tilde{\tau}_2$ mass to 5 GeV from the endpoint of the τ -jet energy spectrum as illustrated in Fig. 13.

Production cross section for both these modes can be determined at the level of 4%, and the polarization of τ -leptons from the $\tilde{\tau}_1$ decay, which gives access to the $\tilde{\tau}$ and $\tilde{\chi}_1^0$ mixing⁵, could be measured with an accuracy better than 10%, eg. from $\tau \rightarrow \pi^+ \nu_\tau$ decays. Fig. 14 illustrates an additional possibility to determine the τ -polarization from decays to ρ -mesons ($\tau \rightarrow \rho^+ \nu_\tau \rightarrow \pi^+ \pi^0 \nu_\tau$). In this case, the observable $R = E_\pi / E_{jet}$ can be used to measure the τ -polarization to $\pm 5\%$ by a fit of the templates in Fig. 14 to the data.

3.2.2 Final States with Electrons and Missing Four-momentum

As already illustrated by Fig. 11, the selectron pair production cross section is huge in our scenario due to the t -channel neutralino exchange, allowing a very precise determination of the masses and polarised cross sections in a short time. They give important information on the neutralino mixing, since eg. in case of light higgsinos the t -channel would be strongly suppressed by the small electron Yukawa coupling. In particular, if both beams are given right-handed polarizations, only the $e^+e^- \rightarrow \tilde{e}_R \tilde{e}_L$ process is possible. As this reaction proceeds exclusively via neutralino exchange in the t -channel, it's size gives insight to the neutralino mixing [25].

3.2.3 Final States with Muons and Missing Four-momentum

Figure 15 shows the muon energy distribution for all events with two muons from SM and SUSY processes, before any selection in full simulation of the ILD detector. The striking peak in the SM distribution at the beam energy originates from $e^+e^- \rightarrow \mu^+ \mu^-$. The SUSY contributions (scaled only by a factor of 10 or 100 to be visible at this fully inclusive stage) arise from $\tilde{\mu}_L \tilde{\mu}_L \rightarrow \mu \mu \tilde{\chi}_1^0 \tilde{\chi}_1^0$, $\tilde{\chi}_1^0 \tilde{\chi}_2^0 \rightarrow \mu \mu \tilde{\chi}_1^0 \tilde{\chi}_1^0$ as well as $\tilde{\mu}_R \tilde{\mu}_R$,

⁵Interaction of sfermions and gauginos conserve chirality, while the Yukawa interaction of the higgsinos flips chirality.

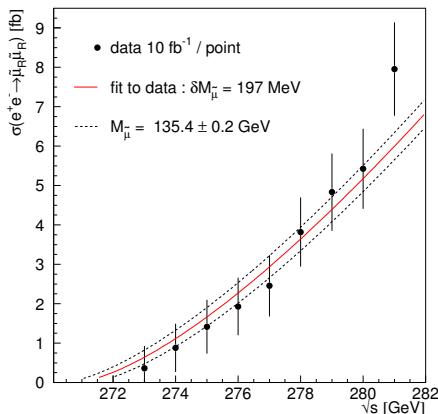


Figure 12: Threshold scan at the $e^+e^- \rightarrow \tilde{\mu}_R\tilde{\mu}_R$ threshold. From Ref. [23]

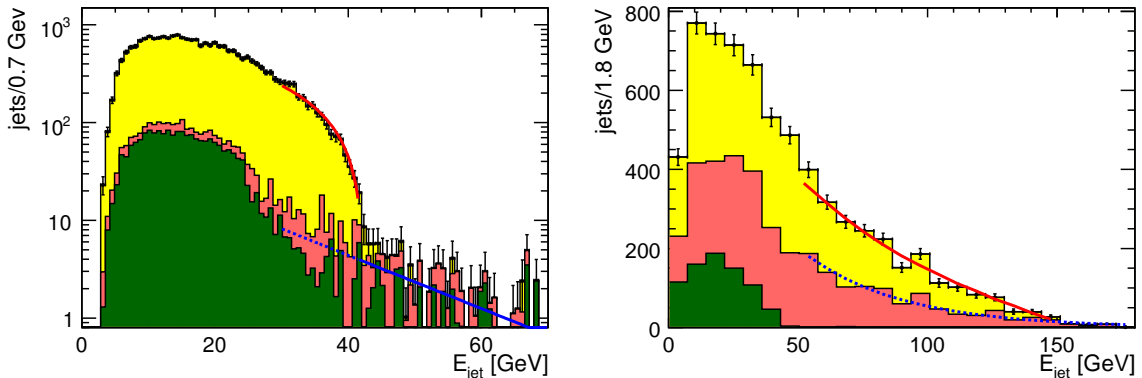


Figure 13: Left: $\tilde{\tau}_1$ spectrum (yellow) and background (SM: red, other SUSY: green), with end-point fit. Right: $\tilde{\tau}_2$ spectrum (yellow) and background (SM: red, other SUSY: green), with end-point fit. From Ref. [24].

$\tilde{\tau}_1\tilde{\tau}_1$ with τ decays to muons and others. We will show in the following that all these contributions can be disentangled and identified.

For the $\tilde{\mu}_L$ case, Fig 16 shows zooms into the edge regions of the muon energy spectrum after a dedicated selection. From the edge positions, the $\tilde{\mu}_L$ mass can be determined to 400 MeV [26].

The even smaller contribution from $\tilde{\chi}_1^0\tilde{\chi}_2^0 \rightarrow \mu\mu\tilde{\chi}_1^0\tilde{\chi}_1^0$ (scaled by factor 100 in inclusive plots) can also be identified, eg. in the invariant mass spectrum of the two muons, as illustrated by Fig 17. From this channel alone, the mass of the $\tilde{\chi}_2^0$ can be determined to a precision of about 1 GeV, depending on the assumed precision for the mass of $\tilde{\mu}_R$ and $\tilde{\chi}_1^0$.

A particularly interesting channel is $e^+e^- \rightarrow \tilde{\chi}_2^0\tilde{\chi}_2^0$ and the $\tilde{\chi}_2^0$ decay to $\tilde{\mu}_R\mu$ (or equivalently to $\tilde{e}_R e$), even if the branching ratio is at the level of a few percent like in our example point. These cascade decays can be fully kinematically constrained at the ILC, and would promise to yield even lower uncertainties on the $\tilde{\mu}_R$ and \tilde{e}_R masses than the threshold scans, of the order of 25 MeV. This is estimated on an earlier study in a scenario with about twice as large branching ratios for the considered decay mode, where a precision of 10 MeV [27] was found. The corresponding distribution of the reconstructed $\tilde{\mu}_R$ mass is shown in the left part of Fig. 18, including all SM and SUSY backgrounds. Even the dominating decays to $\tilde{\tau}_1\tau$ can be constrained as shown in the right part of Fig. 18, and could yield comparable results to a threshold scan.

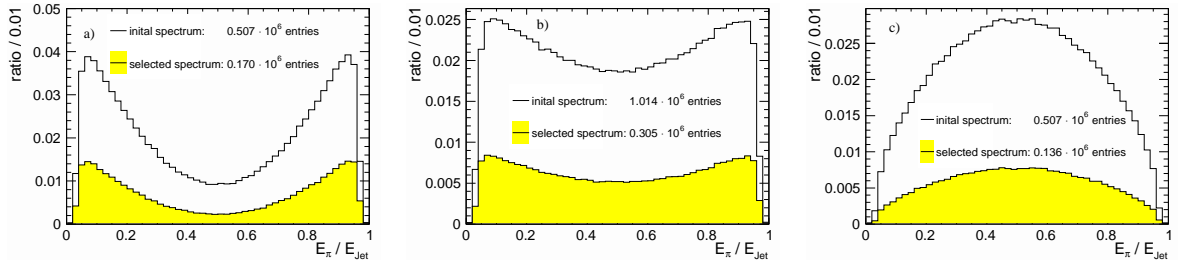


Figure 14: Distribution of the observable $R = E_\pi/E_{jet}$ before (open histogram) and after event selection (grey (yellow) histogram). a): both τ leptons are right-handed. c): the τ leptons have opposite helicity. r): both τ leptons are left-handed. From [24].

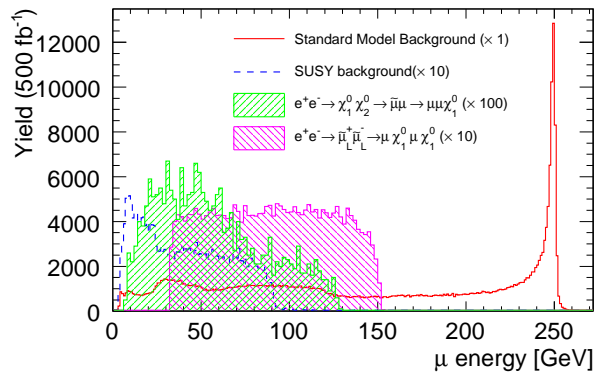


Figure 15: Inclusive muon energy spectrum from di-muon events. From [26].

4 Dark Matter Relic Density

A final goal would be to perform a closure test on the neutralino Dark Matter hypothesis. This can be achieved by using all available collider observables to determine the SUSY parameters and to predict the relic density based on the assumption that the $\tilde{\chi}_1^0$ is the only contribution to Dark Matter.

This has been studied in [28] for the SPS1a scenario, which is very similar to our benchmark points apart from the squarks and gluinos. This means that the projections used for the LHC observables might be too optimistic for the much heavier colored sector in our scenario. This might be partially cancelled by the fact that pre-LHC projections turned out to be rather conservative in many cases. However for the prediction of the relic density, the colored sector is of less importance, while it depends crucially on the electroweak sector, and in particular the LSP and $\tilde{\tau}_1$ properties, which are almost identical between SPS1a' and our scenarios.

Figure 19 shows the relic density obtained in mSugra and MSSM18 fits to many toy experiment outcomes of LHC and ILC measurements. It shows that the ILC measurements allow to predict $\Omega_{\text{CDM}} h^2$ in the MSSM18 case almost as precisely as in mSugra with only 4 free parameters (and one sign) in stead of 18 parameters. The LHC alone would leave a comparison with cosmological observations at an inconclusive and thus unsatisfactory level. This example beautifully illustrates the complementarity of the two machines.

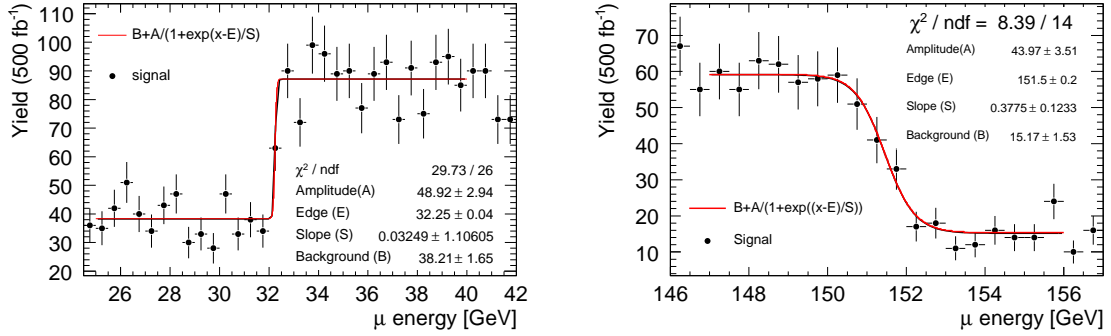


Figure 16: Determination of the $\tilde{\mu}_L$ mass from edges in the muon energy spectrum. Left: lower edge; Right: upper edge. From [26].

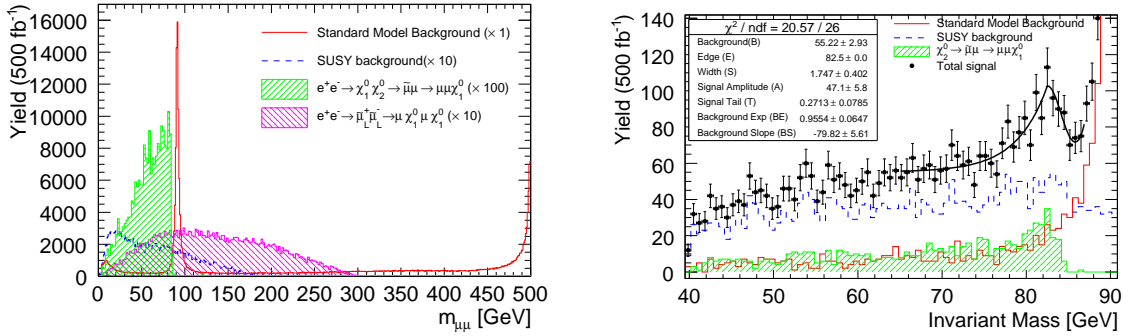


Figure 17: Determination of the $\tilde{\chi}_2^0$ mass the di-muon invariant mass spectrum Left: full spectrum for inclusive di-muon sample; Right: zoom into signal region after dedicated selection. From [26].

5 Conclusions

We have presented a series of $\tilde{\tau}$ -coannihilation scenarios based on the pMSSM, which is compatible with all known experimental constraints. It illustrates that the phenomenology of full models can be significantly more subtle than suggested by the simplified model approach. Especially the \tilde{t}_1 masses of this series, ranging from ~ 300 to ~ 700 GeV seem to be excluded by current LHC limits in simplified models. However we showed that due to many different long decay chains the actual analyses are not yet sensitive to these scenarios.

At LHC14, the observability of the considered model points in terms of a deviation from the Standard Model depends strongly on the systematic uncertainty on the background. In fully hadronic stop searches or stop searches with one lepton, STC4, STC5 and STC6 could be discovered provided that the systematic uncertainty on the background does not exceed about 20%. Discovery of STC8 as well as electroweakino production in any of the scenarios requires systematic uncertainties at the few percent level. Larger statistics, like the LHC high-lumi running (3000 fb^{-1}) can be exploited only if the systematic uncertainties are low enough, roughly in the few percent region. While the stop searches are rather robust against pileup, the effect of considering 50 pileup events is clearly visible in the electroweakino searches. The simulation results with 140 pileup events support these observations (appendix 6.3)

For the scenarios with lighter stop masses, stop pair production amounts up to $\sim 90\%$ of the total SUSY cross section. At the 2nd highest considered stop mass, electroweakino production is already dominant. We could

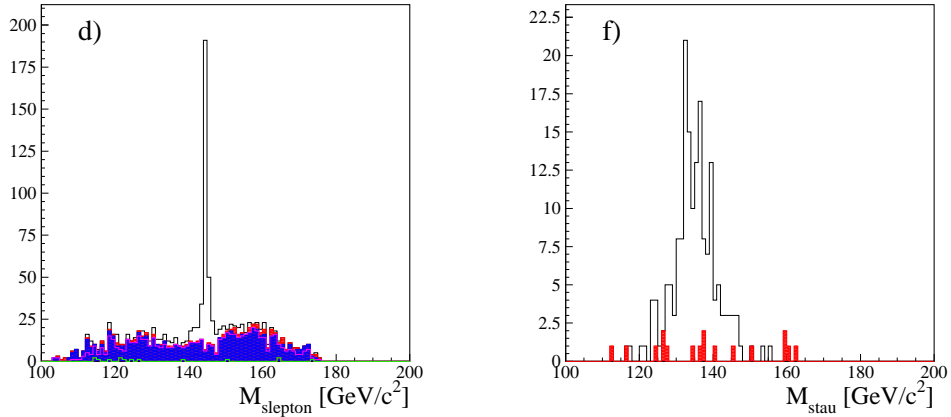


Figure 18: Reconstruction of slepton masses from $\tilde{\chi}_2^0\tilde{\chi}_2^0 \rightarrow \tilde{l}\tilde{l}$ in SPS1a, which has a very similar spectrum to our case. Left: reconstructed $\tilde{\mu}_R$ mass. Right: reconstructed $\tilde{\tau}_1$ mass. From [27].

not yet investigate how well contributions from these and other open channels (eg. sbottom production) can be disentangled from each other and how well properties of individual sparticles can be measured.

At the ILC, nearly all sleptons and electroweakinos are accessible either in pair or associated production, several of them would be most likely discoveries in view of the LHC studies summarised above. We gave a brief summary of some of the existing studies on spectroscopy in our scenario(s) and also older studies of points with a very similar electroweak part of the spectrum, like SPS1a' or SPS1a. In particular for SPS1a it has been shown in previous studies that ILC precision is mandatory to achieve a satisfactory precision on the predicted Dark Matter relic density.

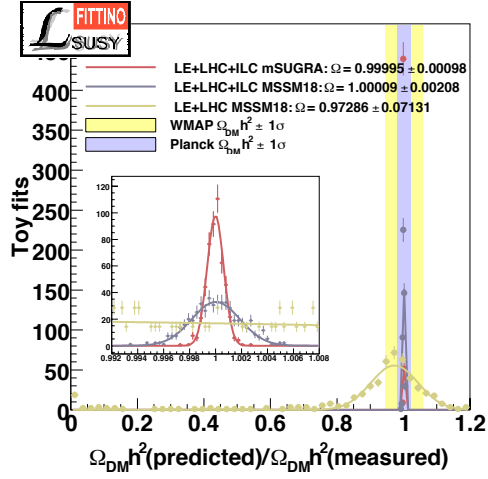


Figure 19: Ratio of the predicted value of $\Omega_{\text{pred}}h^2$ to the nominal value of $\Omega_{\text{SPS1a}}h^2$ in the SPS1a scenario for a variety of Fittino Toy Fits without using $\Omega_{\text{CDM}}h^2$ as an observable. From [28]. The anticipate predictions for LHC and ILC measurements are compared to current and projected cosmological observations.

References

- [1] O. Buchmueller, R. Cavanaugh, A. De Roeck, J. Ellis, H. Flacher, *et al.*, “Likelihood Functions for Supersymmetric Observables in Frequentist Analyses of the CMSSM and NUHM1,” *Eur.Phys.J.* **C64** (2009) 391–415, [arXiv:0907.5568 \[hep-ph\]](#).
- [2] **ATLAS** Collaboration, ATLAS Collaboration, “Search for direct-slepton and direct-chargino production in final states with two opposite-sign leptons, missing transverse momentum and no jets in 20 fb⁻¹ of pp collisions at $\sqrt{s} = 8$ tev with the atlas detector,” ATLAS Conference Note ATLAS-CONF-2013-049, 2013. <http://cds.cern.ch/record/1546777>.
- [3] **CMS** Collaboration, CMS Collaboration, “Search for direct ewk production of susy particles in multilepton modes with 8tev data,” CMS Physics Analysis Summary CMS-PAS-SUS-12-022, 2012. <http://cds.cern.ch/record/1546777>.
- [4] H. Baer and J. List, “Post LHC8 SUSY benchmark points for ILC physics,” [arXiv:1307.0782 \[hep-ph\]](#).
- [5] T. Sjostrand, S. Mrenna, and P. Z. Skands, “PYTHIA 6.4 Physics and Manual,” *JHEP* **0605** (2006) 026, [arXiv:hep-ph/0603175 \[hep-ph\]](#).
- [6] W. Beenakker, R. Hopker, M. Spira, and P. Zerwas, “Squark and gluino production at hadron colliders,” *Nucl.Phys.* **B492** (1997) 51–103, [arXiv:hep-ph/9610490 \[hep-ph\]](#).
- [7] W. Beenakker, M. Kramer, T. Plehn, M. Spira, and P. Zerwas, “Stop production at hadron colliders,” *Nucl.Phys.* **B515** (1998) 3–14, [arXiv:hep-ph/9710451 \[hep-ph\]](#).
- [8] **ATLAS** Collaboration, ATLAS Collaboration, “Search for direct stop pair production in events with missing transverse momentum and two b-jets in 12.8 fb⁻¹ of pp collisions at $\sqrt{s} = 8$ tev with the atlas detector,” ATLAS Conf Note ATLAS-CONF-2013-001, 2013. <http://cds.cern.ch/record/1503233>.
- [9] M. L. Graesser and J. Shelton, “Hunting Asymmetric Stops,” *Phys.Rev.Lett.* **111** (2013) 121802, [arXiv:1212.4495 \[hep-ph\]](#).
- [10] S. Ovin, X. Rouby, and V. Lemaitre, “DELPHES, a framework for fast simulation of a generic collider experiment,” [arXiv:0903.2225 \[hep-ph\]](#).
- [11] A. Avetisyan *et al.*, “Snowmass Energy Frontier Simulations for Hadron Colliders,” [arXiv:1307.XXX \[hep-ph\]](#).
- [12] A. Avetisyan *et al.*, “Standard Model Background Generation for Snowmass using Madgraph,” [arXiv:1307.XXX \[hep-ph\]](#).
- [13] M. Cacciari, G. P. Salam, and G. Soyez, “FastJet User Manual,” *Eur.Phys.J.* **C72** (2012) 1896, [arXiv:1111.6097 \[hep-ph\]](#).
- [14] **ATLAS** Collaboration, ATLAS Collaboration, “Search for scalar bottom pair production in final states with missing transverse momentum and two b-jets in pp collisions at $\sqrt{s} = 8$ tev with the atlas detector,” ATLAS Conf Note ATLAS-CONF-2012-165, 2012. <http://cds.cern.ch/record/1497668>.
- [15] G. Polesello and D. R. Tovey, “Supersymmetric particle mass measurement with the boost-corrected contranverse mass,” *JHEP* **1003** (2010) 030, [arXiv:0910.0174 \[hep-ph\]](#).
- [16] **CMS** Collaboration, CMS Collaboration, “Search for top-squark pair production in the single lepton final state in pp collisions at 8 tev,” CMS Physics Analysis Summary CMS-PAS-SUS-13-011, 2013. <http://cdsweb.cern.ch/record/1547550>.
- [17] Y. Bai, H.-C. Cheng, J. Gallicchio, and J. Gu, “Stop the Top Background of the Stop Search,” *JHEP* **1207** (2012) 110, [arXiv:1203.4813 \[hep-ph\]](#).

- [18] **CMS** Collaboration, CMS Collaboration, “Search for electroweak production of charginos, neutralinos, and sleptons using leptonic final states in pp collisions at $\sqrt{s} = 8$ tev,” CMS Physics Analysis Summary CMS-PAS-SUS-12-022, 2012. <http://cdsweb.cern.ch/record/1546777>.
- [19] **ATLAS** Collaboration, ATLAS Collaboration, “Search for direct slepton and gaugino production in final states with hadronic taus and missing transverse momentum with the atlas detector in pp collisions at $\sqrt{s} = 8$ tev,” ATLAS Conf Note ATLAS-CONF-2013-028, 2012. <http://cds.cern.ch/record/1525889>.
- [20] C. Bartels, *WIMP Search and a Cherenkov Detector Prototype for ILC Polarimetry*. PhD thesis, University of Hamburg, <http://www-flc.desy.de/flc/work/group/thesis/doctor.2011.bartels.pdf>, 2011.
- [21] S. Caiazza, “Measuring the selectron properties at the ILC,” in *ECFA LC2013*. 2013.
- [22] C. Bartels, O. Kittel, U. Langenfeld, and J. List, “Measurement of Radiative Neutralino Production,” [arXiv:1202.6324](https://arxiv.org/abs/1202.6324) [[hep-ph](#)].
- [23] J. E. Brau, R. M. Godbole, F. R. L. Diberder, M. Thomson, H. Weerts, *et al.*, “The Physics Case for an e+e- Linear Collider,” [arXiv:1210.0202](https://arxiv.org/abs/1210.0202) [[hep-ex](#)].
- [24] P. Bechtle, M. Berggren, J. List, P. Schade, and O. Stempel, “Prospects for the study of the $\tilde{\tau}$ -system in SPS1a’ at the ILC,” *Phys.Rev.* **D82** (2010) 055016, [arXiv:0908.0876](https://arxiv.org/abs/0908.0876) [[hep-ex](#)].
- [25] G. Moortgat-Pick, T. Abe, G. Alexander, B. Ananthanarayan, A. Babich, *et al.*, “The Role of polarized positrons and electrons in revealing fundamental interactions at the linear collider,” *Phys.Rept.* **460** (2008) 131–243, [arXiv:hep-ph/0507011](https://arxiv.org/abs/hep-ph/0507011) [[hep-ph](#)].
- [26] N. D’Ascenzo, *Study of the Neutralino Sector and Analysis of the Muon Resoponse of a Highly Granular Hadron Calorimeter at the International Linear Collider*. PhD thesis, University of Hamburg, <http://www-library.desy.de/cgi-bin/showprep.pl?desy-thesis-09-004>, 2009.
- [27] M. Berggren, “Reconstructing sleptons in cascade-decays at the linear collider,” in *Proceedings of LCWS04*, pp. 907–910. Paris, April, 2004. [arXiv:hep-ph/0508247](https://arxiv.org/abs/hep-ph/0508247) [[hep-ph](#)].
- [28] P. Bechtle, K. Desch, M. Uhlenbrock, and P. Wienemann, “Constraining SUSY models with Fittino using measurements before, with and beyond the LHC,” *Eur.Phys.J.* **C66** (2010) 215–259, [arXiv:0907.2589](https://arxiv.org/abs/0907.2589) [[hep-ph](#)].

6 Appendix

6.1 Resolution of the jet momentum

We investigate the jet momentum for the three different pileup scenarios. Reconstructed jets are matched to generator level jets with the criterium $\Delta R < 0.5$, where the distance parameter $\Delta R = \sqrt{\Delta\eta^2 + \Delta\phi^2}$ is used to match the closed generator level jet. We define the resolution as $(p_T^{\text{gen}} - p_T^{\text{rec}})/p_T^{\text{gen}}$.

Figure 20 contains the comparison for the hardest jet and for all jets with the reconstructed momentum $p_T > 30$ GeV. The jet resolution decreases with higher pileup. Figure 21 shows a similar plot for the E_T^{miss} resolution. The generator level information contains all objects that are invisible for the detector, like neutrinos or neutralinos. Also the E_T^{miss} resolution decreases with increasing pileup as expected.

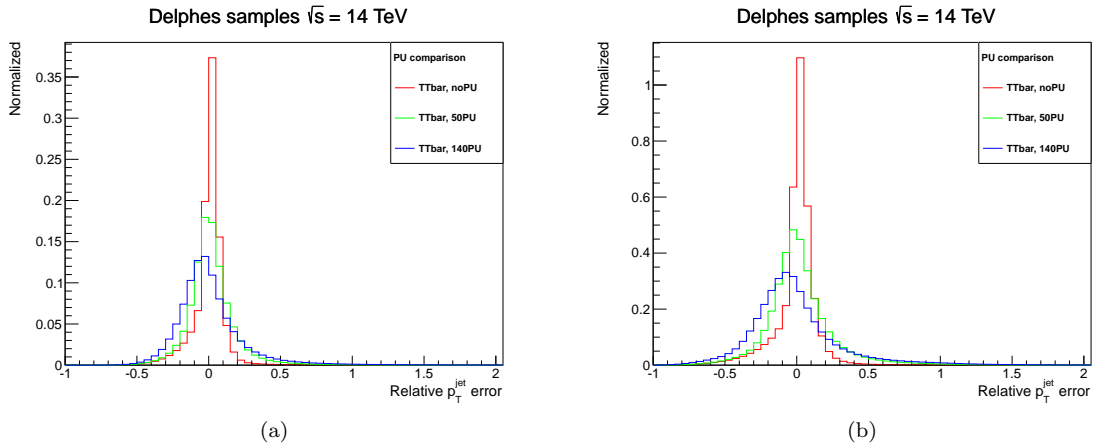


Figure 20: Comparison of the reconstructed and generated p_T for simulated $t\bar{t}$ events with 0, 50 PU and 140 PU events for the hardest (a) and all jets (b). Shown is in both cases the resolution, for the definition see text.

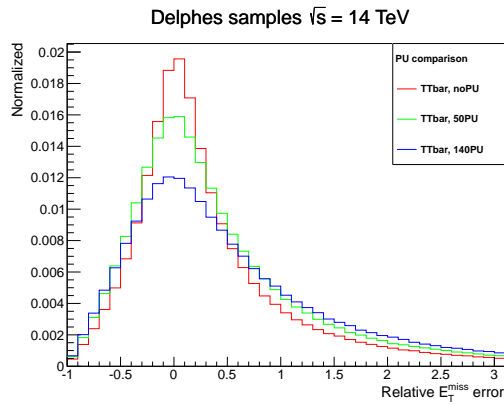


Figure 21: Comparison of the reconstructed and generated E_T^{miss} for simulated $t\bar{t}$ events with 0, 50 PU and 140 PU events.

6.2 Comparison of signal cross sections

The main production processes at the LHC running at a center-of-mass energy of 14 TeV are summarized in Table 10. The subprocess with the largest cross section in model STC4 is direct stop production. The stops predominantly decay to top quarks and the lightest neutralino (54%), or to bottom quarks and the lightest chargino (46%). Here, the chargino decays mainly to tau and neutrino (70 %), suggesting analyses searching for tops in the final state, either with one or no lepton.

The mass of the stop quarks rises from model STC4 to STC8 subsequently from 293 GeV to 750 GeV, reducing the cross section for stop production significantly, while the production cross section of the electroweak particles stays roughly the same. The latter are very hard to identify at the LHC, as they mainly decay to final states containing tau leptons.

Table 10: Overview over the cross sections of the main processes calculated at leading order by Pythia at the LHC with a center-of-mass energy of 14 TeV

Model	Process	Relative cross section	LO cross section from Pythia
	$gg \rightarrow \tilde{t}_1 \tilde{t}_1$	70%	5.2 pb
	$gg \rightarrow \tilde{b}_1 \tilde{b}_1$	0.1%	11 fb
	$q\bar{q} \rightarrow \tilde{t}_1 \tilde{t}_1$	9.4%	0.70 pb
STC4	$q\bar{q} \rightarrow \chi_1^+ \chi_2^0$	8.0%	0.61 pb
	$q\bar{q} \rightarrow \chi_1^- \chi_2^0$	4.5%	0.34 pb
	$q\bar{q} \rightarrow \chi_1^+ \chi_1^-$	6.5%	0.49 pb
	$gg \rightarrow \tilde{t}_1 \tilde{t}_1$	31%	0.73 pb
	$gg \rightarrow \tilde{b}_1 \tilde{b}_1$	0.6%	12 fb
	$q\bar{q} \rightarrow \tilde{t}_1 \tilde{t}_1$	6.2%	0.15 pb
STC5	$q\bar{q} \rightarrow \chi_1^+ \chi_2^0$	25%	0.64 pb
	$q\bar{q} \rightarrow \chi_1^- \chi_2^0$	13%	0.32 pb
	$q\bar{q} \rightarrow \chi_1^+ \chi_1^-$	20%	0.48 pb
	$gg \rightarrow \tilde{t}_1 \tilde{t}_1$	10%	0.18 pb
	$gg \rightarrow \tilde{b}_1 \tilde{b}_1$	0.6%	11 fb
	$q\bar{q} \rightarrow \tilde{t}_1 \tilde{t}_1$	2.9%	0.05 pb
STC6	$q\bar{q} \rightarrow \chi_1^+ \chi_2^0$	36%	0.63 pb
	$q\bar{q} \rightarrow \chi_1^- \chi_2^0$	19%	0.33 pb
	$q\bar{q} \rightarrow \chi_1^+ \chi_1^-$	27%	0.48 pb
	$gg \rightarrow \tilde{t}_1 \tilde{t}_1$	1.1%	18 fb
	$gg \rightarrow \tilde{b}_1 \tilde{b}_1$	0.7%	12 fb
STC8	$q\bar{q} \rightarrow \chi_1^+ \chi_2^0$	40%	0.63 pb
	$q\bar{q} \rightarrow \chi_1^- \chi_2^0$	21%	0.33 pb
	$q\bar{q} \rightarrow \chi_1^+ \chi_1^-$	31%	0.49 pb

6.3 Cutoffs for the scenario with 140 pileup events and 3000 fb^{-1}

The following pages show the cutflows for simulations with 140 pileup events. The selections are identical to the three cases discussed in section 2. Some of the cuts are adapted to the larger statistics assuming 3000 fb^{-1} at 14 TeV.

Table 11: Outflow: number of events for the inclusive signal samples and several important backgrounds for the full-hadronic stop analyses with 3000 fb^{-1} at 14 TeV with 140 pileup events. The last two lines show the significances with an additional systematic background uncertainty of 25% and, as an optimistic scenario, of 15%.

Description	diboson	ttbar+jets	boson+jets	single top	sum bgrds	STC4	STC5	STC6	STC8
preselection	1108210000	2161240000	168402000000	620665000	172292115000	38400000	11460000	7590000	6570000
lepton veto	940242000	1487090000	159642000000	502288000	162571620000	28679700	8447620	5632630	4994540
n jets ≥ 3	201104000	1183240000	32492600000	233184000	34110128000	16757100	3284950	1229670	691336
jet1 > 120 GeV	74779600	546969000	8058930000	94522500	8775201100	9572540	2458540	846769	375882
jet2 > 70 GeV	65339800	510834000	6852930000	81913300	7511017100	8493500	2223710	749506	304717
jet3 > 60 GeV	41908700	415604000	3625730000	50266400	4133509100	6533640	1738650	590349	218424
bjets <i>ge2</i>	3372470	230206000	195456000	17357200	446391670	3424080	1012000	341458	101420
$H_T > 1000 \text{ GeV}$	265364	12417600	8318720	631840	21633524	494592	179313	83465	43579
$\Delta\Phi > 0.5$	178354	8002890	5590080	405644	14176968	303096	131683	65378	35453
$E_T^{miss} / m_{eff} > 0.2$	5599	157699	115775	6005	285079	138792	61382	33273	19742
$E_T^{miss} > 1000 \text{ GeV}$	240	540	4569	27	5378	5976	3769	2999	2944
$s/\sqrt{b + (0.25 * b)^2}$						4.4	2.8	2.2	2.2
$s/\sqrt{b + (0.15 * b)^2}$						7.4	4.7	3.7	3.6

Table 12: Cutoff: number of events for the inclusive signal samples and several important backgrounds for the single-lepton stop analyses with 3000 fb^{-1} at 14 TeV with 140 pileup events. The last two lines show the significances with an additional systematic background uncertainty of 25% and, as an optimistic scenario, of 15%.

Description	dlboson	ttbar+jets	boson+jets	single top	sum bgnds	STC4	STC5	STC6	STC8
preselection	1108210000	2161240000	168402000000	620665000	172292115000	38400000	11460000	7590000	6570000
singl. lep. and τ veto	94640200	400316000	5212300000	74380700	5781636900	4348510	1114500	618297	447906
n jets ≥ 4	4732320	102106000	136368000	4329060	247535380	1562500	356513	141841	52116
b-tagged jets = 1 or 2	1419280	81610600	31314400	3294970	117639250	1201010	270116	97023	26776
$E_T^{miss} > 500$ GeV	4893	67767	39029	2269	113958	25608	12892	8471	4266
$\Delta\Phi > 0.5$	4504	59682	36012	1865	102065	17616	10618	7290	3876
$H_T > 1500$ GeV	547	6403	4165	150	11266	4968	2802	1830	1400
$M_T > 120$ GeV	76	1103	367	19	1566	2760	1674	1218	866
topness > 9.5 and p_T asym. < -0.2	48	628	222	13	913	1632	1208	881	710
$H_T > 1750$ GeV	24	313	119	6	463	1128	868	605	525
$s/\sqrt{b} + (0.25 * b)^2$						9.6	7.4	5.1	4.5
$s/\sqrt{b} + (0.15 * b)^2$						15.5	11.9	8.3	7.2

Table 13: Cutoff: number of events for the inclusive signal samples and several important backgrounds for the same-sign di-lepton analysis targeting electroweak particles with 3000 fb^{-1} at 14 TeV and with 140 pileup events. The last two lines show the significances with an additional systematic background uncertainty of 30% and, as an optimistic scenario, of 20%.

Description	dlboson	ttbar+jets	boson+jets	single top	sum bgnds	STC4	STC5	STC6	STC8
preselection	1108210000	2161240000	168402000000	620665000	172292115000	38400000	11460000	7590000	6570000
2 lepton req.	19295000	67454200	514871000	1627920	603248120	977736	443583	329663	250383
$E_T^{miss} > 120$ GeV	1867680	12033600	20908400	270240	35079920	478392	249524	180581	124423
same-sign req.	112615	74246	59914	20679	267455	21504	28238	24820	17714
Z veto	49880	73564	38490	20675	182610	18792	23296	19795	14597
b-jet veto	42453	21839	30696	10652	105641	10272	10573	8850	7986
$E_T^{miss} > 200$ GeV	8951	4132	6989	1437	21511	4992	5452	4927	4401
$E_T^{miss} > 400$ GeV	944	218	857	81	2102	1152	1316	1377	1170
$s/\sqrt{b} + (0.3 * b)^2$						1.8	2.1	2.2	1.9
$s/\sqrt{b} + (0.2 * b)^2$						2.7	3.1	3.3	2.8